ANALYSIS OF THERMAL TRANSPORT IN MINICHANNEL HEAT SINKS

By

KALYAN PANKAJ INAMDAR

A thesis submitted to the

Graduate School New Brunswick

Rutgers, The State University of New Jersey

In partial fulfilment of the requirements

For the degree of

Master of Science

Graduate Program in Mechanical and Aerospace Engineering

Written under the direction of

Prof. Yogesh Jaluria

And approved by

_____

_____

_____

New Brunswick, New Jersey

October 2017

ABSTRACT OF THE THESIS

ANALYSIS OF THERMAL TRANSPORT IN MINICHANNEL HEAT SINKS

By Kalyan Inamdar

Thesis Director: Prof. Yogesh Jaluria

Many biological systems providing very high heat and mass transfer rates in organs such as brain, liver, and lungs use microchannels and minichannels. A few years back transport in small channels gained ground due to the high heat transfer rates. Since then a lot of research has been done on heat transfer in microchannels both experimentally and numerically. The analysis done minichannels is mainly experimental and very less literature exists on numerical analysis done on heat transfer in minichannels. Some work that exists, considers short channels with aspect ratios in the range of 0.3 to 0.5. Moreover, the work done prior to this work considered considerably lower imposed heat fluxes. The experimental work done on minichannel heat sinks also considers short sinks with

heat flux in the order of 40kW/m^2. Hence, in this study the focus is on minichannels with an aspect ratio of the order of 0.01 and with very high heat flux imposed, of the order of 700 kW/m^2. The analysis is done for three as well as two-dimensional channels. Three different channels of height 1 mm, 2 mm and 3 mm are analyzed and the results of the analysis are studied. The pressure drop across the heat sink is also reported. The temperature drop across the heat sink is reported and found to be minimum for the channel with height 3 mm for a three-dimensional channel.

Acknowledgements

First and foremost, I would like to extend my gratitude towards Professor Jaluria. He has been extremely patient and supportive. Personally, for me, he is a great source of inspiration and I admire his dedication towards his work and teaching. Courses taught by him are the most informative and fun, and I enjoyed taking two courses under him. I am most thankful for his patience and understanding. I will always remember the very wide spectrum of conversations we have had.

I express my gratitude to all the professors under whom I took courses. All of them are very ardent in their work and are very helpful. I would also like to thank my friends and fellow students Saumil, Ridhish and Saurabh. I admire their passion towards their work and the perfection with which they both want to accomplish something. I will always cherish the wide spectrum of conversations with Saumil. I wish them all the luck in their future endeavors.

Last but not the least I would like to express my gratitude towards the Khandekar family, without them, this would not have been possible.

Dedication

This thesis is dedicated to my parents; they are a great source of inspiration.

TABLE OF CONTENTS

LISTOF FIGURES

NOMENCLATURE

A	Area, m^2
C_p	Specific heat (kJ/kg °C)
D_h	Hydraulic diameter (m)
Eu	Euler Number- $Phigh- Plow/\rho V2$
f_f	Friction factor
h	Heat transfer coefficient (W/m^2K)
k	Thermal conductivity (W/ m K)
L	Length of the channel (mm)
Nu	Nusselt Number - $h\ Dh/k$
P	Power Density (W/ m^2)
ΔP	Pressure Drop (Pa)
q	Heat flux (W/ m^2)
Q	Flow rate ($m3/ s$)
r_h	Hydraulic radius (m)
Re	Reynolds number - $\rho\ V\ D_h/\mu$
T_{out}	Temperature of coolant at the outlet (°C)
T_{in}	Temperature of coolant at inlet (°C)
T_{base}	Base Temperature of heat sink (°C)
u	Velocity (m/s)
V	Characteristic Velocity of the Flow (m/s)
W	Width (mm)

Greek Symbols

Δ	Difference
μ	Dynamic Viscosity (kg/ m-s)
ϑ	Kinematic Viscosity (m^2/s)
θ	Dimensionless Temperature
β	Thermal expansion coefficient (K^{-1})
ρ	Density (kg/m^3)

Chapter 1: Introduction

A lot of research is being carried out currently in the field of minichannels. It has been proven that minichannels and microchannels are very effective methods for thermal transport than conventional methods. Moreover, more and more research is being done to further enhance the heat transfer in minichannels by various methods like using different fluids, variations in geometry etc. However, not a lot of work has been done to analyze the effectiveness of the long minichannels for very high heat flux, which will be the focus of this study.

1.1 Literature Review

Xie et al. (2007) carried out a numerical investigation on the fluid flow and heat transfer in minichannel heat sinks for a chip with an active cooling area of 20 mm x 20 mm. They concluded that pressure drop is highly dependent on the channel geometry, and the heat transferred in a deep and narrow channel is better that a shallow and wide channel. Saad et. al.[1] investigated different heat sinks of five different fin spacing of 0.2 mm, 0.5 mm, 1 mm and 1.5 mm. It was concluded that for the fin spacing with the least dimension i.e. 0.2 mm the lowest base temperature was achieved. As a result, the conclusion obtained by Xie et al.[2] is verified. Kandlikar and Dharaiya [3] studied the effect of structured roughness on enhancement of heat transfer in minichannels and microchannels experimentally as well as numerically. A significant enhancement in heat transfer of approximately 250% was found with a channel separation of 550 microns with a roughness height of 20 microns. Moreover, they observed that the flow remained laminar and no vortices were generated mainly

because the roughness elements were structured in a sinusoidal waveform and were smooth. A sharp element will further increase the heat transfer but at the expense of increased pressure head. Moreover, it was also concluded from their study that freely available fluid, water has a lot of potential to be used as coolant in high heat generating devices, and its potential should be completely exploited before looking at other fluids like the nanofluids. Moreover, other mechanisms such as flow boiling, multiphase flows can enhance the heat transfer considerably. Balasubramanian and Kandlikar[4] studied the flow patterns, pressure drop and flow instabilities in parallel rectangular minichannels with hydraulic diameter of 333 μm. Nucleate boiling was observed in the bulk liquid flow as well as in the thin liquid film surrounding the vapour slug. This confirmed the dominance of nucleate boiling heat transfer. Further slug flow was observed to be dominant for higher surface temperatures. This further confirms the conclusion that heat transfer can be enhanced by methods other than using nanofluids like modifying the flow. Flow modification is an important aspect that can be employed to enhance heat transfer before looking for any other options.

As mentioned above another aspect of thermal management is enhanced liquid cooling by improving the thermophysical properties of the fluids. Xuan and Li [5] used a hot-wire to measure thermal conductivity. For example, for the water-Cu nanoparticles suspension the thermal conductivity ratio varies from 1.24 to 1.78 if the volume fraction of ultra-fine particles increases from 2.5% to 7.5%. The volume fraction, shape, dimensions and properties of the nanoparticles affect the thermal conductivity of the nanofluids. Similarly, Choi et al. [6] found thermal conductivity enhancement of 160% with a concentration of 1% of carbon nanotubes by volume. Many such works have reported increased thermal conductivities and hence enhanced heat transfer, when using fluids added with nanoparticles in working fluids. There are some issues reported for using nanofluids like high

maintenance, high cost, aggregation and deposition on the surfaces of the channels etc. However, not much research has gone into analysis of heat transfer and fluid flow characteristics of minichannels for use in applications such as providing cooling for machining process or for energy harvesting, for example use in solar power collectors. This study focuses on applications such as these.

1.2 Motivation

Channels of small diameters are at the heart of all biological systems. For example, the human body utilizes high heat and mass transfer coefficients. Taking inspiration from nature, many devices utilize micro and minichannels, for applications such as cooling of electronics, energy harvesting. One such application for minichannel can be imagined in the form of device which is used in solar panels to absorb the irradiation, with flow boiling, may later be converted to some other form of energy.

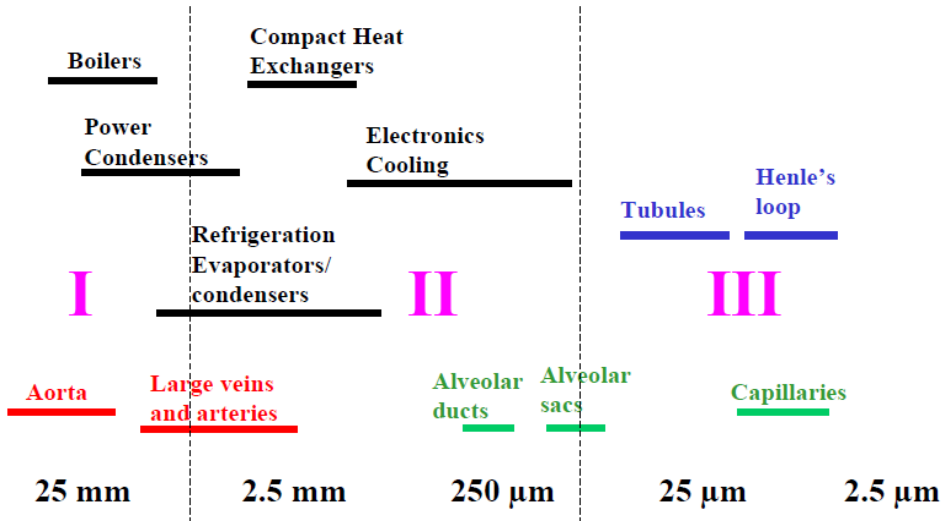

Figure 1: Ranges of channel diameters employed in various applications, Kandlikar S. G. [7]

Figure 1, given by Kandlikar[7], shows some key biological systems along with the progression of heat exchanger technology toward the microscale arena.

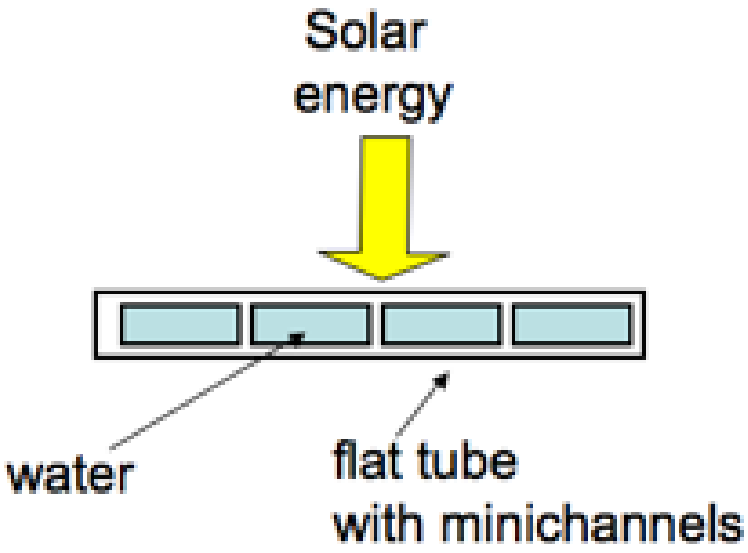

Figure 2: Minichannels used for the application of energy harvesting

The channels as shown here can be used effectively for applications such as energy harvesting for example in solar panels. The channels as shown above can be manufactured very easily as well as investigated experimentally by Vembuli [8]. In his thesis, Vembuli investigated heat transfer in minichannels manufactured by a simple milling process. Such channels are not expensive and are even widely available commercially. Cooling of a machining process for example grinding process, in which a huge amount of energy is generated, can also be achieved using minichannels. The use of microchannels is not recommended in such applications because very often the scale of these applications is in the mini or macro range. For example for cooling a slab of metal 100 mm by 100 mm, using a series of microchannels will not be effective since a large number of channels will be required, also the length of the channels will have to be on the macro scale. This will effectively, make the pressure drop very high to be handled by low power and low cost easily available commercial pumps. For such cases therefore, minichannels can be used very effectively compared to microchannels. Another such example is an array of Vertical Cavity Surface Emitting Lasers (VCSELs), which is used in applications such as virtual reality, which heat comparable to an electronic chip. In this case, as well use of minichannels is preferred.

The main objective of this work is to analyze the heat transfer and fluid flow in minichannels under moderate to high heat flux. Furthermore, the aspect ratio of the channel is higher than which has been seen in previous works, in the order of 0.01. Most often in such cases, water is used as the working fluid, which is available easily and is cost effective. Hence, in this investigation water will be used as the working fluid to determine the effectiveness of the minichannels for thermal transport applications.

Chapter 2: Modelling Aspects and Implementation

2.1 Introduction

Water is the most easily available fluid in nature, inexpensive and non-toxic. In some cases, tap water can also be used as the operating fluid but that has some disadvantages like contaminants, some of which can even be macro-sized. However, most cooling systems use distilled water as the working fluid. In this study as well working fluid is water at 30 ^{0}C. The variation in properties of water for a wide temperature range is not considerable and hence for the properties of water are considered constant. Moreover, the heat capacity of water is much more than that of air, which is also one of the widely used fluids for cooling. However, special care needs to be taken if water is used for electronics cooling then special care needs to be taken to protect the electronics from water. Having said that, for applications like solar panels or cooling of machining processes water is the most efficient fluid to be used as the working fluid.

For the analysis of the thermal and flow, calculations the following assumptions are made:

1. The flow is three-dimensional, incompressible, steady and laminar.
2. The effect of body force is neglected.
3. Thermo-physical properties of the working fluid are constant.

The numerical simulation was done on the entire computational domain. In the solid region, the energy equation is solved, considering that the velocities go to zero and only conduction

effects remain. In the following section, the equations solved, the assumptions and the boundary conditions employed are delineated.

2.2 Mathematical Model

For rectangular minichannels normally used the aspect ratio, W / H is not very high, unlike the microchannels used in various applications. Hence, in case of minichannels where the aspect ratio W / H ≈ 1, a two-dimensional model cannot be employed. Therefore, all the equations are needed to be solved in three dimensions. However, in some cases the applications requires the width of the channel be very high compared to its height, and hence a two-dimensional model can be employed. The schematic of the three-dimensional and two-dimensional models are shown in Figures 2 and 3 respectively.

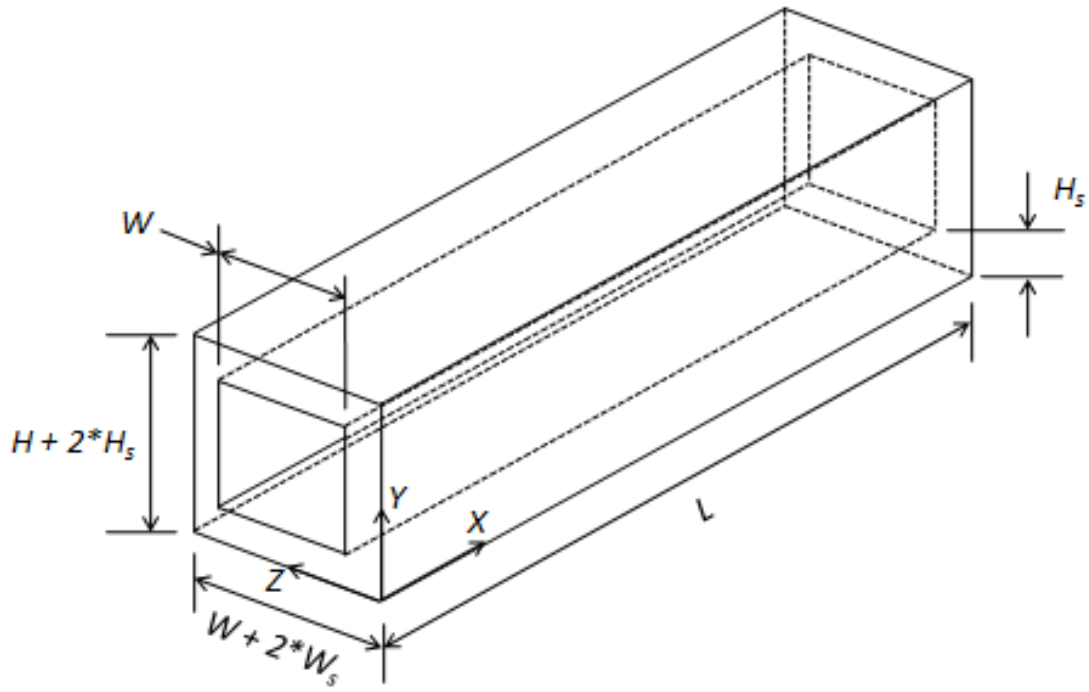

Figure 3: Schematic of a 3D rectangular channel and coordinate system

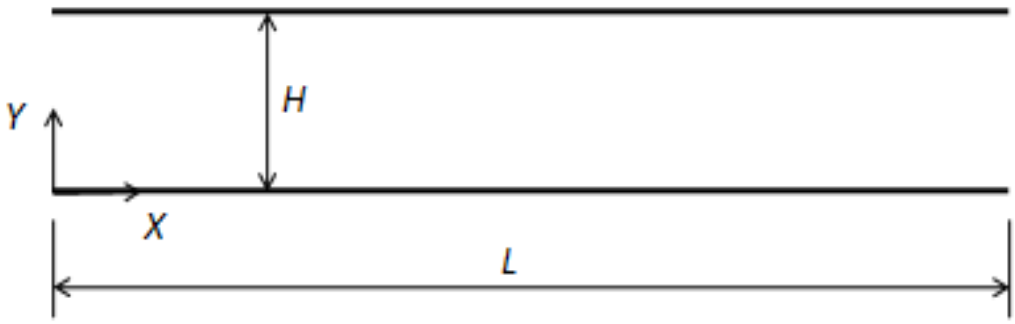

Figure 4: Schematic of rectangular 2D channel and coordinate system

Continuity and the full elliptic Navier-Stokes equations are given below. Given the non-linearity of the Navier-Stokes equations, a predictor-corrector method is needed to be employed. A predictor-corrector method uses guessed initial velocity field, which is then used to compute the pressure field. This pressure field is then used to calculate the pressure corrections to correct the velocity. The procedure is repeated until convergence is reached.

The governing equations are:

Continuity:

$$\frac{\partial \rho u}{\partial x} + \frac{\partial \rho v}{\partial y} + \frac{\partial \rho w}{\partial z} = 0$$

Momentum:

$$\frac{\partial \rho u u}{\partial x} + \frac{\partial \rho v u}{\partial y} + \frac{\partial \rho w u}{\partial z} = -\frac{\partial p}{\partial x} + \frac{\partial}{\partial x}\left(\mu \frac{\partial u}{\partial x}\right) + \frac{\partial}{\partial y}\left(\mu \frac{\partial u}{\partial y}\right) + \frac{\partial}{\partial z}\left(\mu \frac{\partial u}{\partial z}\right)$$

$$\frac{\partial \rho u v}{\partial x} + \frac{\partial \rho v v}{\partial y} + \frac{\partial \rho w v}{\partial z} = -\frac{\partial p}{\partial y} + \frac{\partial}{\partial x}\left(\mu \frac{\partial v}{\partial x}\right) + \frac{\partial}{\partial y}\left(\mu \frac{\partial v}{\partial y}\right) + \frac{\partial}{\partial z}\left(\mu \frac{\partial v}{\partial z}\right)$$

$$\frac{\partial \rho u w}{\partial x} + \frac{\partial \rho v w}{\partial y} + \frac{\partial \rho w w}{\partial z} = -\frac{\partial p}{\partial z} + \frac{\partial}{\partial x}\left(\mu \frac{\partial w}{\partial x}\right) + \frac{\partial}{\partial y}\left(\mu \frac{\partial w}{\partial y}\right) + \frac{\partial}{\partial z}\left(\mu \frac{\partial w}{\partial z}\right)$$

Energy:

$$\frac{\partial \rho u T}{\partial x} + \frac{\partial \rho v T}{\partial y} + \frac{\partial \rho w T}{\partial z} = \frac{\partial}{\partial x}\left(k\frac{\partial T}{\partial x}\right) + \frac{\partial}{\partial x}\left(k\frac{\partial T}{\partial y}\right) + \frac{\partial}{\partial x}\left(k\frac{\partial T}{\partial z}\right) + \mu\Phi$$

Where $\mu\Phi$ is the viscous dissipation and the pressure work is neglected.

In the energy equation, given above, the convection terms are non-linear, if buoyancy or variable properties are considered, and are needed to be solved with the predictor-corrector method. However, in this study, the properties of water are considered constant and hence the equations are not coupled. As a result, the equations can be solved to obtain the velocity field first and then the energy equation can be solved to obtain the temperatures.

In the cases where a heat flux is imposed, conjugate heat transfer arises and convection boundary condition is imposed at the interface of solid and liquid. No-slip boundary condition is adopted at the wall. At the inlet, the distribution of velocity is constant and equal to the inlet velocity as calculated from the Reynolds number for a specific geometry:

x = 0, $u = U_{in}$, $v = w = 0$

x = L, $\frac{\partial u}{\partial x} = 0$

At walls, $u = v = w = 0$

The thermal boundary conditions are as follows,

y = 0, $\frac{\partial T}{\partial y} = 0$

y = W + 2*W_c, $\frac{\partial T}{\partial z} = 0$

y = 0, $-\left(k\frac{\partial T}{\partial y}\right) = q$

y = H + 2*H_c, Adiabatic wall: $\frac{\partial T}{\partial z} = 0$

x = 0, $T = T_{in}$

x = L, $\frac{\partial T}{\partial x} = 0$

According to Patankar[10], coordinates of a computational grid can be classified as one-way or two-way. The convection-diffusion scheme used in this work allows the space coordinate to be one way. When the Peclet number is large the coefficient of a downstream neighbour becomes zero. At the outflow, the scalar values or flux may not be known. However, the Peclet number at the outlet is very large and hence the downstream coefficient becomes very small and negligible and hence the no boundary values will be needed. However, for convenience a fully developed condition at the outlet is employed.

A staggered grid is used for the computational domain and Finite Volume Method (FVM) is used for the solution. Using the method of Thakur and Shyy[9], the Second Order Upwind scheme (SOU) for a uniform grid is derived. The coefficients of First Order Upwind (FOU), as given by Patankar[10], are still applicable in this method, except that an additional term is combined in the source term, to avoid significant false diffusion. All the scalars are computed explicitly. SIMPLER algorithm given by Patankar[10]is used to solve the coupled equations, using Successive Under-Relaxation (SUR) method.

2.3 Validation

Validation and testing of the code to be used for computational analysis. Validation assessment determines if the computational simulation agrees with physical reality. It examines the science in the models through comparison to experimental results or prior

works that have been done on a similar problem. The validation of the code and the mesh used for analysis are discussed in this section.

2.3.1 Mesh

A flexible mesh is used for all the analysis done in this thesis. A flexible mesh means the number of points was not fixed in either direction. The values of Δx, Δy, and Δz i.e. the difference between two grid points in either direction is not fixed and can be varied according to the requirements. Computer memory is an important consideration in any simulation. The cost of resources and the simulation time hugely depends upon the efficient use of computer memory. However, to a reduction in usage of memory by reducing the number of grid points is not advisable as it is necessary to use a sufficiently fine grid to when there is a significant change in the physical quantities to capture the fine changes in the physical quantities. However, when such is not the case, a less refined grid can be used. Hence, a flexible mesh can be a very good resource for the optimal use of resources.

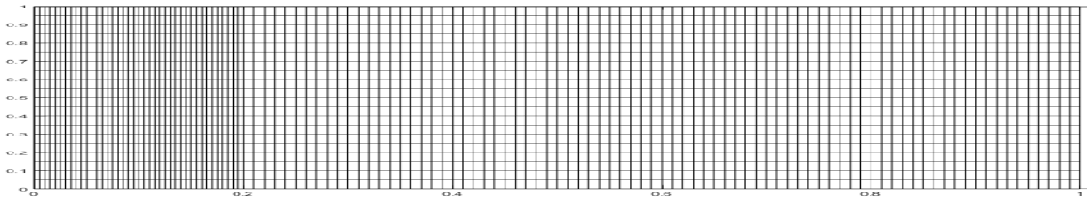

Figure 5: Mesh for channel of height 2 mm and length 100 mm

The mesh for a channel of height 2 mm and length 100 mm is shown in the preceding figure. An initial value of Δx is chosen. This value is the Δx after the boundary layer develops, which is around 20 diameters for the velocity boundary layer. In the developing region, Δx is less than the initial value of the Δx. A mesh with of Δx of 1 mm for the developed region and 0.5 mm for the developing region was found to be sufficiently fine for the analysis.

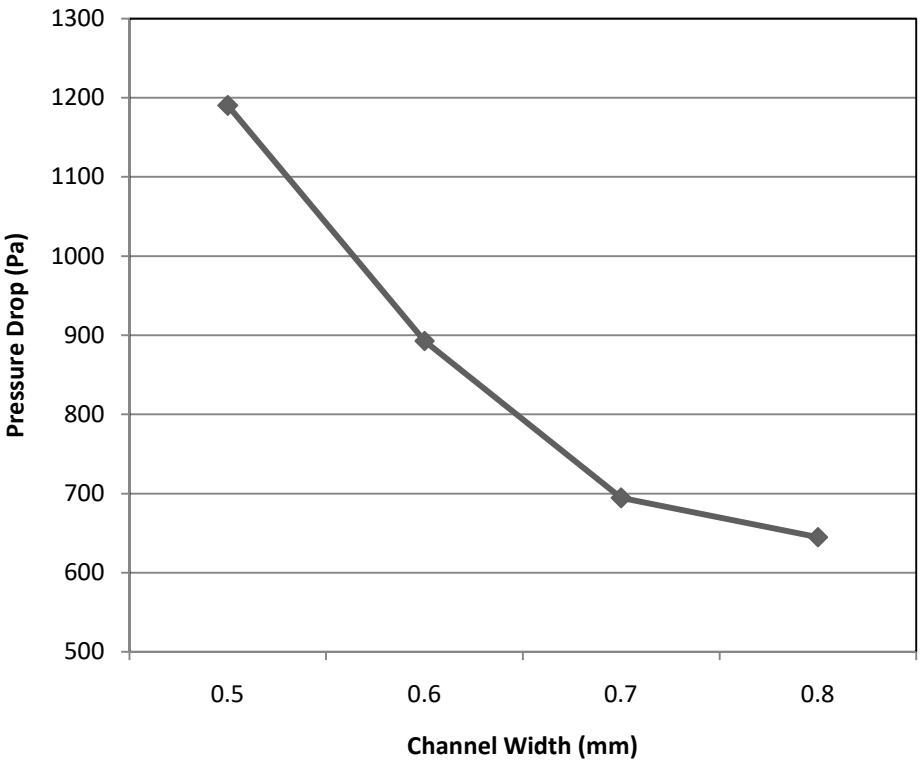

Figure 6: Effect of channel width on pressure drop

Figures 6 and 7 show the effect of channel width on pressure drop obtained by the code written for this thesis and the result obtained by Xie et. Al. (2007).

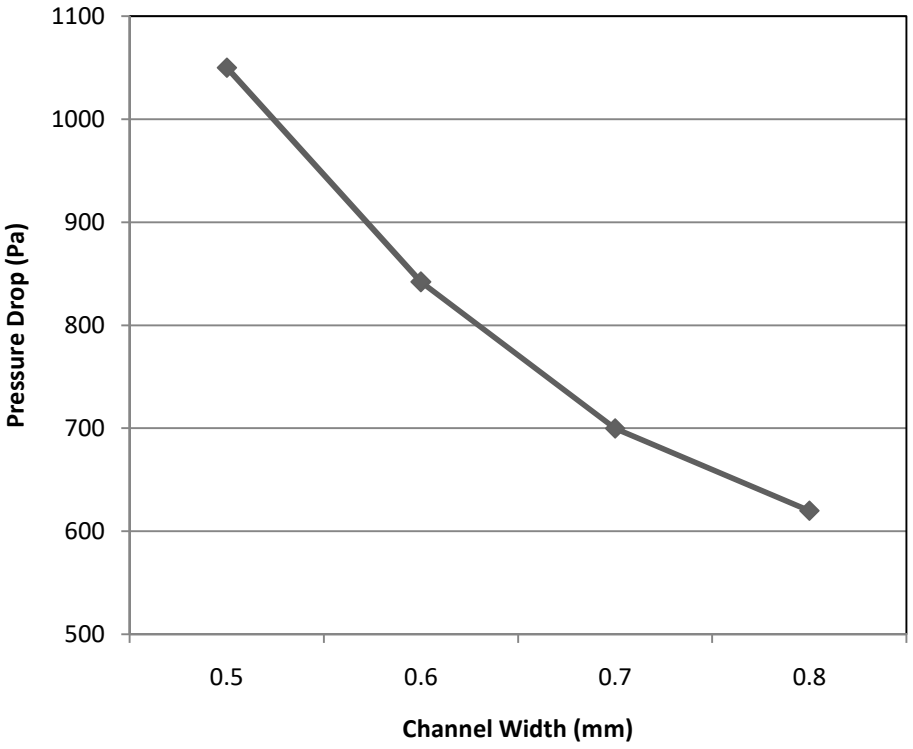

Figure 7: Reproduction of effect of channel width on pressure drop, Xie et al. 2007

Another method to validate a code is to vary the Δx, Δy, and Δz of the mesh grid. Doing this allows to validate the code as well as to determine the dependence of the parameters on grid refinement. Figure number 8 shows the grid dependence test for a channel of hydraulic diameter of 1 mm and an isothermal surface of 50 deg. C. It can be seen that the deviation between the grid (201x21x21) and grid (101x21x21) is not large but is considerable. Hence, for greater refinement grid (201x21x21) is adopted. The grid dependence test also helps validate the code and shows that the code is not dependent on a specific grid.

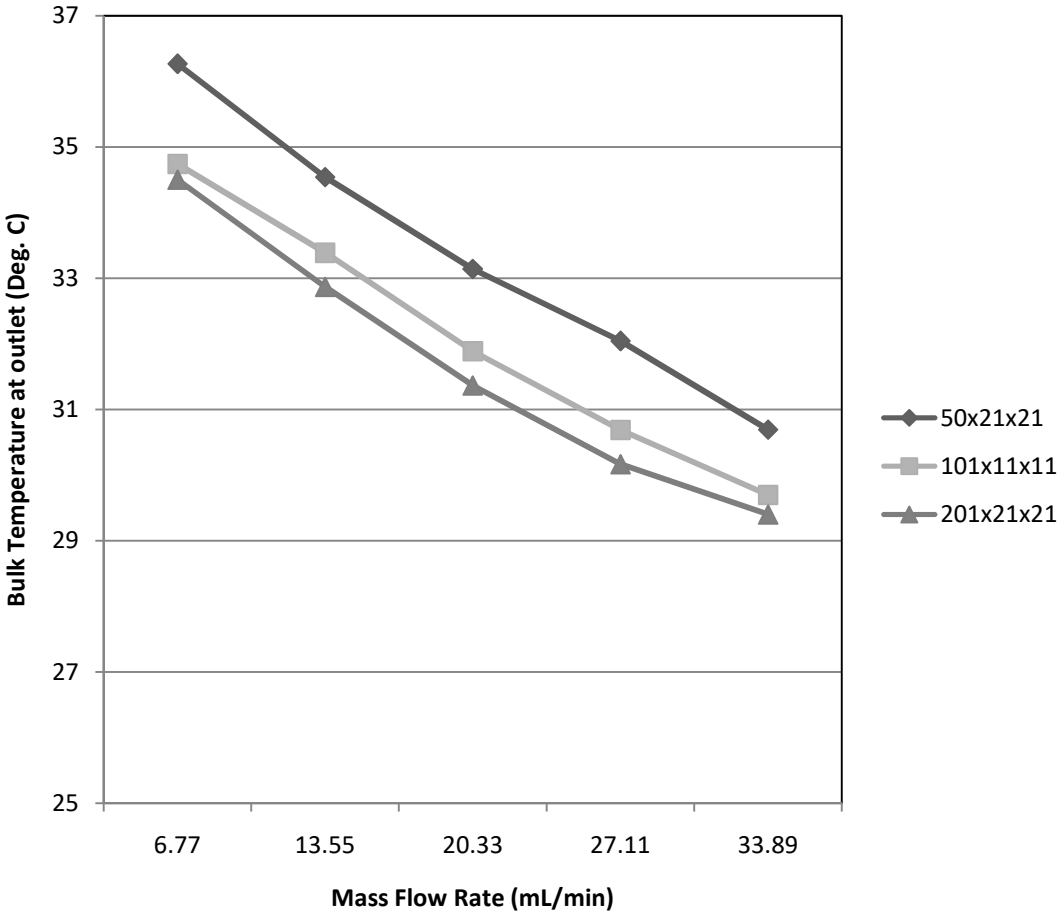

Figure 8: Grid test with the channel of hydraulic diameter 1mm and isothermal surface of 50 Deg. C.

Chapter 3: Results and Discussion

The results obtained from the simulations with the setup explained previously are determined in this chapter. However, before the results are presented, the dimensional numbers and quantities are explained first. Results obtained for various configurations are explained later in this chapter.

3.1 Hydraulic Parameters

The following are the non-dimensional numbers commonly used in fluid mechanics and heat transfer, which are of significance for this study. Non-dimensional numbers can give good physical insight about the nature of the problem. Moreover, varying the parameters shows how the outputs vary with conditions that are controllable by the user.

3.1.1 Reynolds Number

One of the dimensionless parameters that are very useful and important in this study is the Reynolds number. It is given as the ratio of inertial forces to viscous forces.

$$\boldsymbol{Re = \frac{\rho * V * L}{\mu}}$$

Where, $\boldsymbol{V}$is the characteristic velocity of fluid, $\boldsymbol{L}$is the hydraulic diameter and $\boldsymbol{\mu}$is the dynamic viscosity

3.1.2 Euler Number

Euler number is a dimensionless number used in fluid flow calculations. It expresses the relationship between local pressure drop and the kinetic energy per unit volume. It is mainly used to characterize the losses in the flow, where a frictionless flow corresponds to a Euler number of one.

$$Eu = \frac{P_{high} - P_{low}}{\rho * V^2}$$

Where, P_{high} is the pressure at inlet

P_{low} is the pressure at outlet

V is the characteristic velocity of fluid

3.1.3 Theoretical Pressure Drop

It is important to understand how the theoretical pressure drop is calculated. It gives a good idea about the trend and helps us compare the values obtained numerically.

$$\Delta P = f_f * \frac{L}{D} * \rho * V^2$$

Where, ΔP is the pressure drop, L is the length of channel

D is the hydraulic diameter, ρ is the density, and f_f is friction factor

The friction factor is defined as the ratio of wall shear stress τ to the kinetic energy per unit volume. The friction factor for a rectangular channel is given by the following formula,

$$f_f = \frac{64}{Re}$$

The friction factor is not a constant and depends on the hydraulic diameter of the channel and characteristics of fluid like density and characteristic velocity of the flow.

3.1.4 Hydraulic Diameter

Hydraulic diameter provides a method by which non-circular channels can be treated as circular. The need for hydraulic diameter arises due to the use of a single dimension in case of dimensionless quantity like the Reynolds number. The hydraulic diameter allows the use of relationships developed for circular pipes with non-circular channels. The hydraulic diameter can be calculated as follows,

$$D = \frac{4 * A}{P}$$

Where A is the area of cross-section of the channel

P is the perimeter of the cross-section of the channel

3.1.5 Nusselt Number

Nusselt number is defined as the ratio of convective conductance to the pure molecular thermal conductance. In other words, it is the ratio of heat transferred through convection, due fluid motion, to the heat transferred through conduction that is when the heat conducting material is stationary. The Nusselt number provides an idea about the quality of heat transferred rather than the quantity. Nusselt number is defined as,

$$Nu = \frac{h * D}{k}$$

Where $h$isthe convective heat transfer coefficient of fluid

$k$isthermal conductivity of fluid

$D$is the characteristic diameter of the channel

3.2 Analysis of Thermal Transport in Minichannel

The results obtained from the simulations are given below. To validate the code first a flow between parallel plates with isothermal walls is simulated, for various Reynolds numbers and for various temperature ratios (Isothermal temperature/Inlet fluid temperature). This is done to check that the temperature in the system lies between the maximum temperature, i.e. the isothermal temperature and the minimum temperature, i.e. inlet temperature.

The fluid flow of three different configurations of minichannels is discussed here. The results are discussed for flow between flat parallel plates. This analysis includes the comparison of

Reynolds number with Euler number, a variation of Nusselt number with non-dimensional length, a variation of centreline temperature with length.

3.2.1 Fluid Performance

3.2.1.1 Fluid Performance of Two-Dimensional Channel

The fluid performance of the two-dimensional channels is discussed here. This analysis includes the comparison of Euler number with Reynolds number, pressure drop comparison with a flow rate of Reynolds number 10, 100, 200, 300, 400 and 500 for channels of length 60 mm and 100 mm. The variation of centreline velocity is plotted as well.

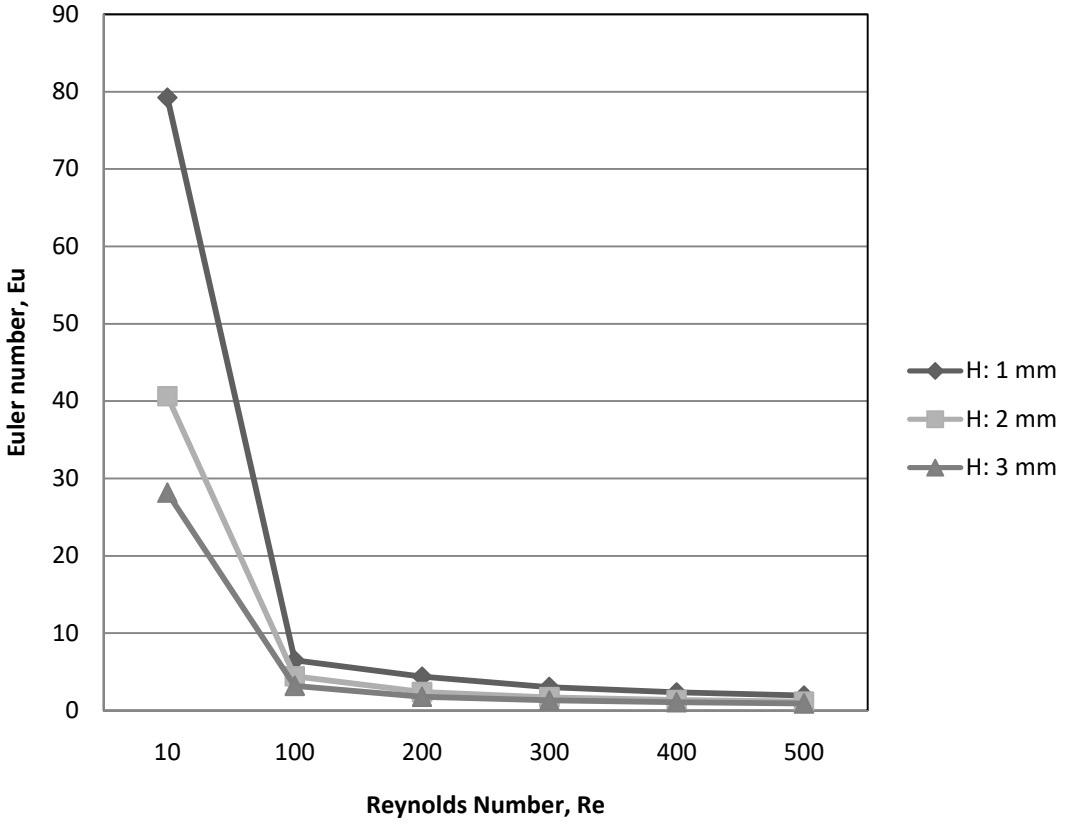

Figure 9: Euler number vs. Reynolds number, channel length 60 mm

The Euler number is used to express the relationship between local pressure drop and the kinetic energy per unit volume. The above figure shows the variation of the Euler number with respect to flow Reynolds number of 10, 100, 200, 300, 400 and 500. It can be seen from the above figure that there is a sharp decrease in the Euler number when going from Reynolds number of 10 to 100 in all the cases. High Euler number usually corresponds to smaller friction factor decreases with increase in the Reynolds number. As the Reynolds number is further increased there was not much change observed in the Euler numbers.

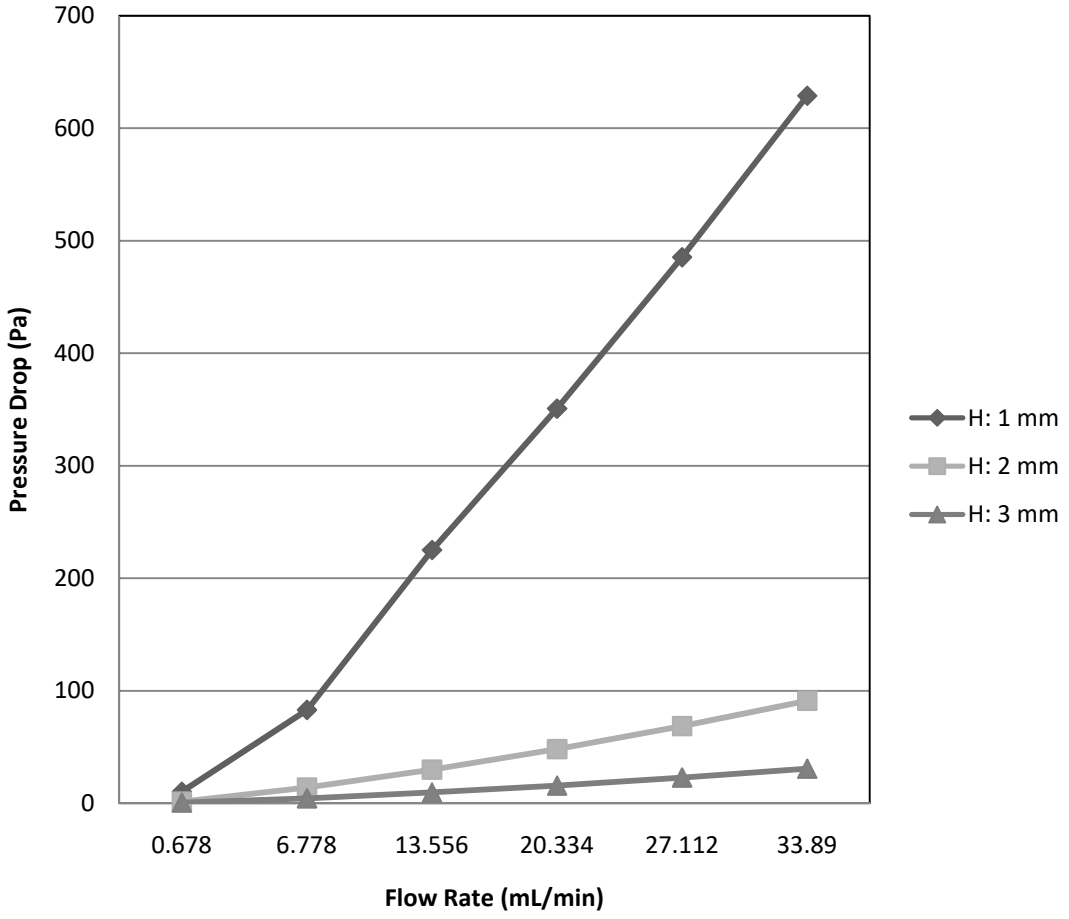

Figure 10: Pressure drop vs. flow rate for a two-dimensional minichannel

This analysis shows the variation of pressure drop with the flow rate. As can be seen the pressure drop has an increasing trend with increasing flow rate, i.e. essentially increasing the

Reynolds number. There is a steep rise in the pressure drop for 1 mm channel, when the flow rate is increased. The maximum pressure drop is 628 Pa for 1 mm channel height and the length is 60 mm. As the height of the channel is increased, the pressure drop decreases and is negligible for channels of 3mm and greater height. The maximum difference in the pressure drop between two geometries is for the flow rate of 33.89mL/min, which is about 610 Pa, between the 1 mm and 3 mm channels. Furthermore, the rate of increase of pressure drop with increasing flow rate is very high for the 1 mm channel compared with the 2 mm and 3 mm channels. Hence, it can be noted that with decreasing channel height the pressure drop will go on increasing with very stark increase in pressure with increasing flow rates.

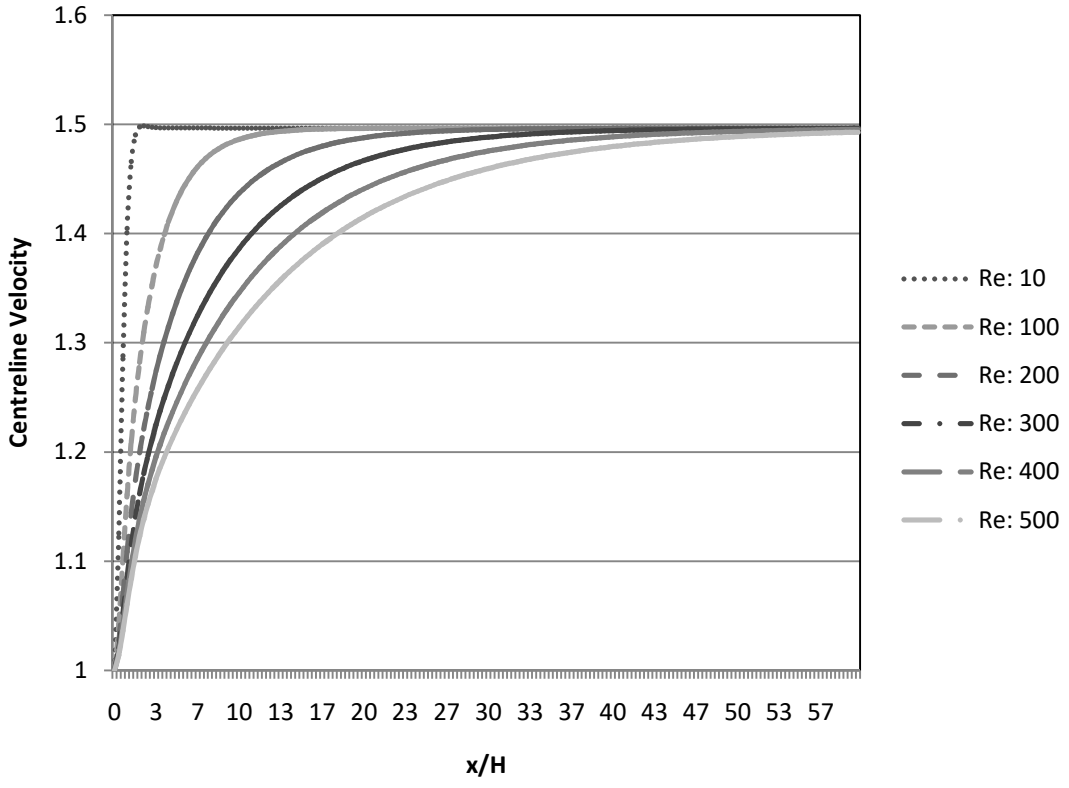

Figure 11: Non-dimensional centreline velocity vs. x/H for channel of height 1 mm

The preceding figure shows the variation of centreline velocity with axial distance. As the Reynolds number is increased, the length required for the flow to develop increases, as can be observed from the above figure. For Reynolds number of 10 the flow develops

immediately while for Reynolds number of 500 the flow just develops towards the end of the channel. With increasing Reynolds numbers the velocity at inlet goes on increasing, if the characteristic diameter is kept the same. Hence, the fluid carries a greater momentum with increasing Reynolds numbers.

3.2.1.2 Fluid Performance of Three-Dimensional Channel

The results for the three-dimensional cases are given below. The results for three types of channels are given below. In each case, the width of the channel remains constant while the height is varied as 1 mm, 2 mm and 3 mm. It is very well known that as the diameter of the channel is reduced the pressure drop increases. However, it is observed that for channels with height 2 mm and 3 mm the differences in Euler numbers are minor. For the pressure drop, though, there is a difference between the two configurations mentioned before at higher Reynolds numbers.

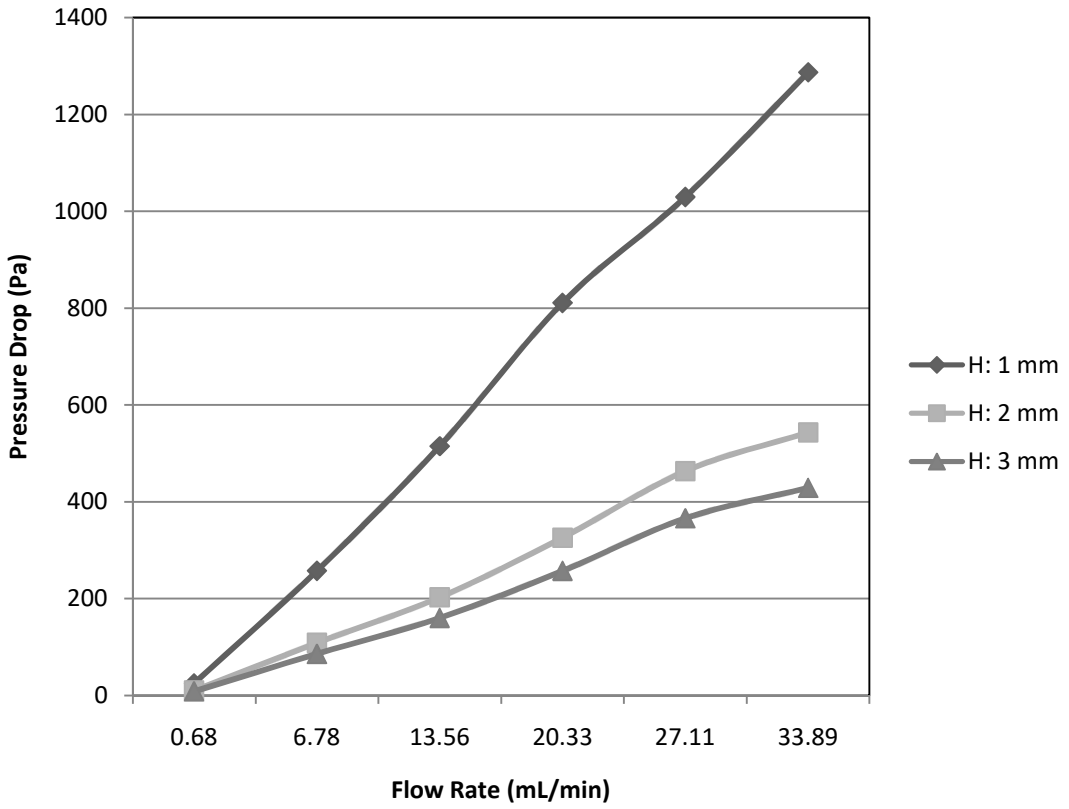

Figure 12: Pressure drop vs. flow rate for a three-dimensional minichannel

Figure 12 shows the pressure drop variation with mass flow/min. It can be observed that the pressure drop for the 1 mm channel increases almost linearly with increasing Reynolds numbers. However, for channels with 2 mm and 3 mm, pressure drop for even the highest flow rate is not considerable compared to the 1 mm channel. Furthermore, the difference between the 2 mm and 3 mm channel for highest flow rate is not 113.9 Pa. For pumps available, commercially this pressure drop can be obtained. Hence, depending upon the capacity of heat removal, which is estimated to be higher for 2 mm channel, the use of 2 mm channel is recommended over the 3 mm channel. When comparing the centreline velocities in the channels at the same flow rates, it is found that the difference is not large. At the same time, it should be kept in mind when selecting a geometry for a minichannel heat sink that the toll of pressure drop is huge when the channel height is reduced from 3 mm to 1 mm.

3.2.2 Thermal Performance

3.2.2.1 Two-Dimensional Channel with Isothermal Surface

As seen before the Nusselt number is a non-dimensional which can be used to determine whether the thermal boundary layer has been developed or not. It is a measure to compare the heat transferred by convection and conduction. Below is the figure showing the Nusselt number for various Reynolds numbers. In this study, a minichannel of length 60 mm is studied for its thermal characteristics. The walls are isothermal and are maintained at a temperature 1.2 times the temperature of the fluid at the inlet, initially.

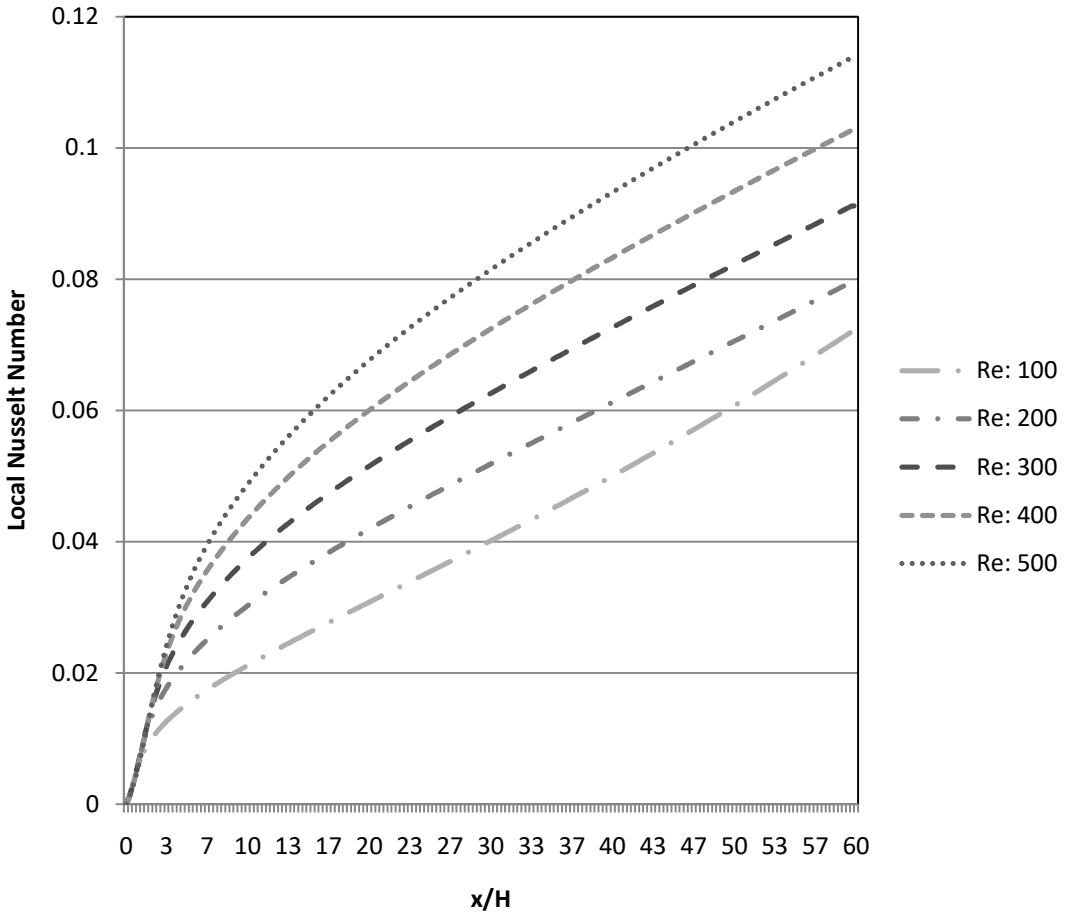

Figure 13: Nusselt number vs. x/H, L: 60 mm, H: 1mm

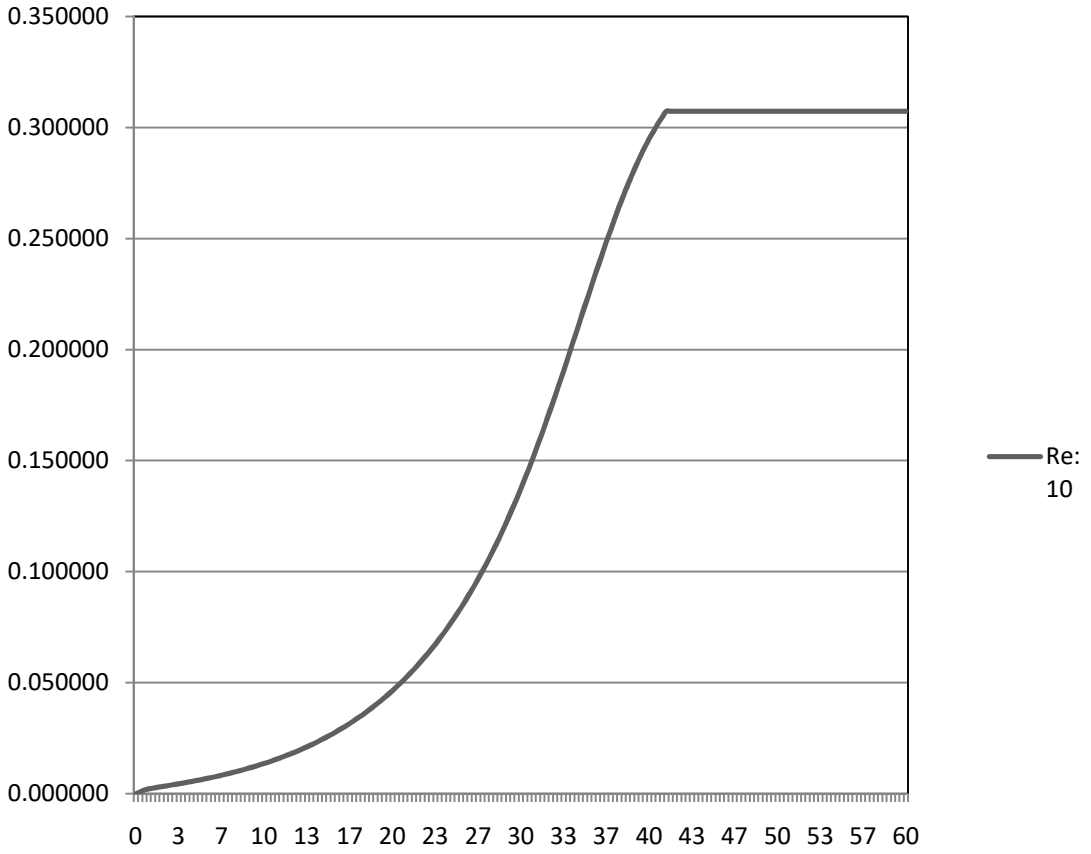

Figure 14: Local Nusselt number vs. x/H, L: 60 mm, H: 1mm, Re 10

By observing the preceding two plots of Nusselt number versus non-dimensional length it can be seen that the thermal boundary layer develops for isothermal boundaries, for a Re of 10, however for the higher Reynolds numbers that is not the case. Hence, for Re 10 increasing the channel length will not increase the heat transfer. Heat transfer can be increased by employing mechanisms such as introducing an obstruction in the channel to break the boundary layer, which will increase the heat transfer Kandlikar and Dharaiya [3].

The following figure shows the variation of Nusselt number versus non-dimensional axial length.

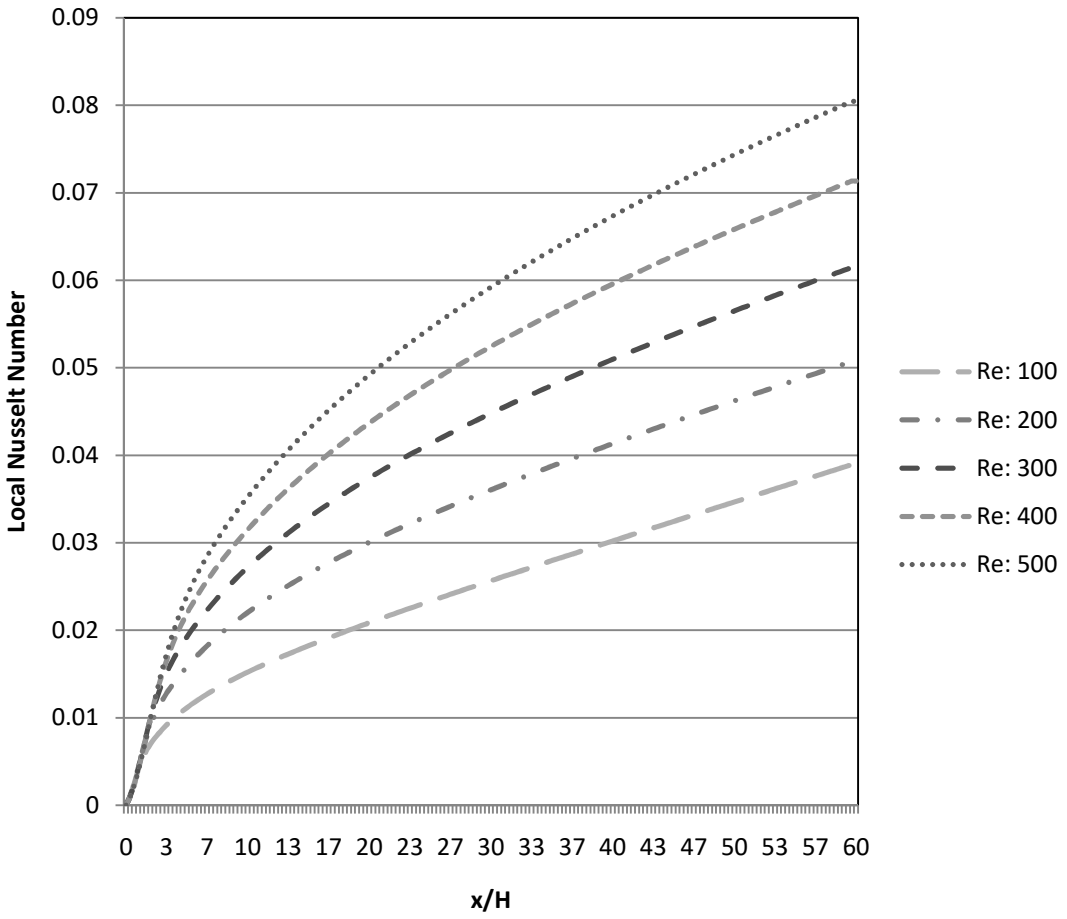

Figure 15: Local Nusselt number vs. x/H, L: 60 mm, H: 2 mm

In this case, the height of the channel is 2 mm. It is expected that the Nusselt number will be less than the Nusselt number for the same case with channel height of 1 mm. However, it can be observed that there is only minor variation in the Nusselt number between the cases of 1 mm and 2 mm. This is expected, the Nusselt number goes on decreasing with increasing Reynolds numbers. For a channel of 2 mm and length, 60 mm for Reynolds number of 100 to 500 does not develop and the analysis can be said to be in the developing region. Further, if the length of the channel is increased the Nusselt number is expected to increase and eventually develop. Figure 10 shows the local Nusselt number with the non-dimensionalised axial length. Compared to the Nusselt number for Reynolds number of 10, it can be seen that there is a large difference. The Nusselt number for Re 10 for 1 mm channel starts to

develop as it nears the end of the channel. However, for the channel with 2 mm height, the Nusselt number just seems to start to develop.

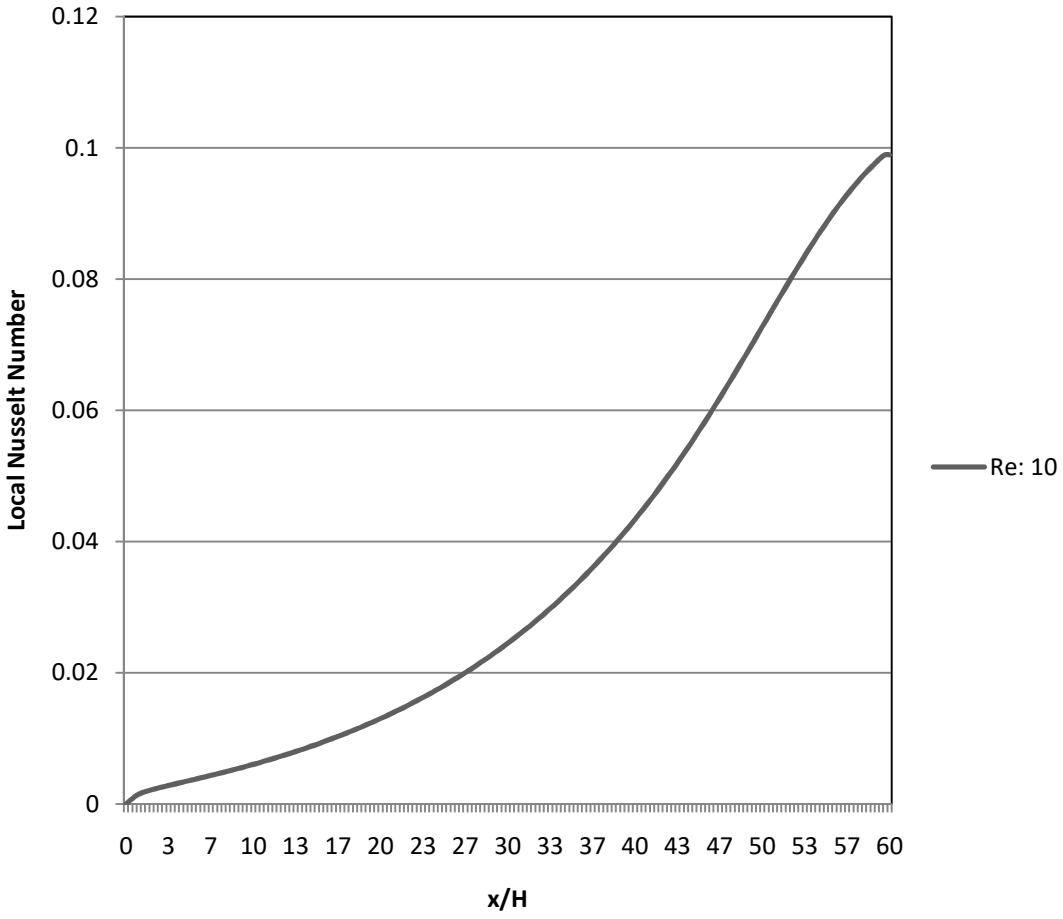

Figure 16: Local Nusselt number vs. x/H, Re: 10, L: 60 mm, H: 2mm

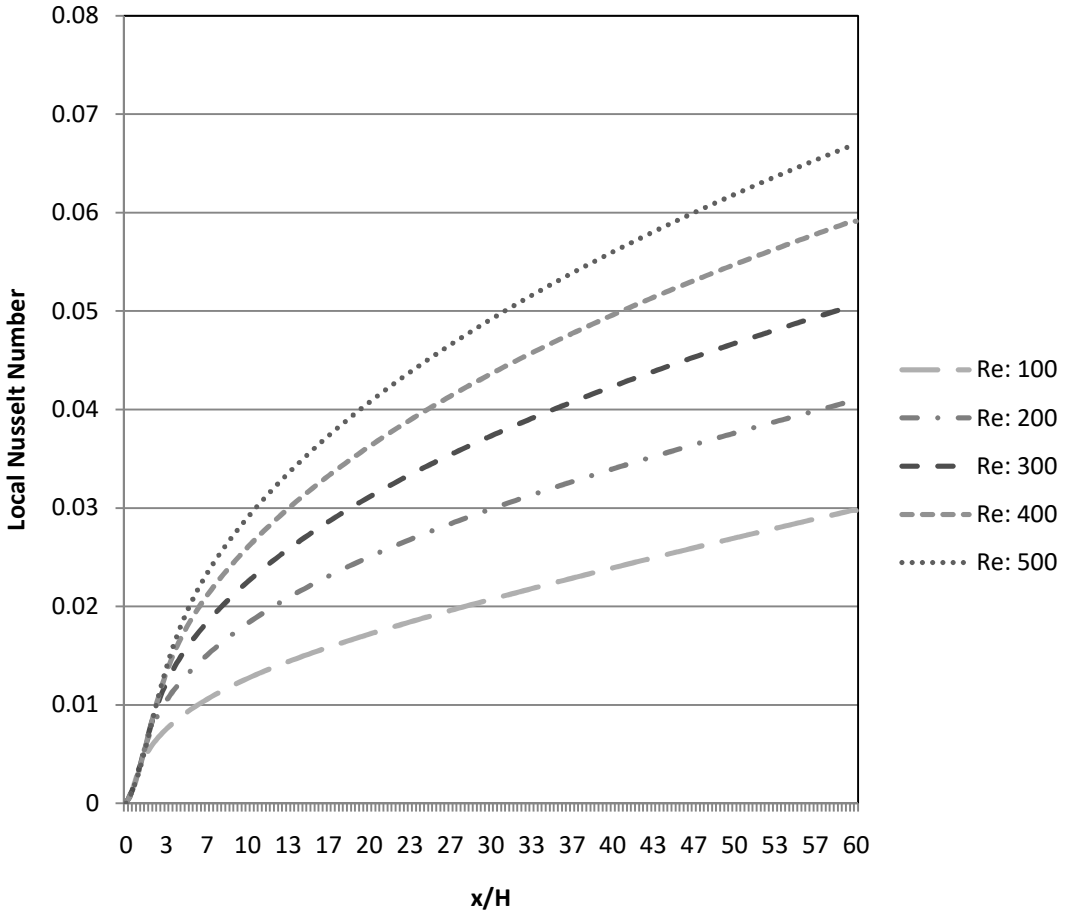

Figure 17: Local Nusselt number vs. x/H

The Nusselt numbers for Reynolds numbers from 100 to 500 are shown for the channel of 3 mm are shown above. Similar to the comparison between the channels of height 1 mm and 2 mm there is only minor difference in the Nusselt number of channel 3 mm and 2 mm. The maximum Nusselt number for the channel with 2 mm height is 0.09; however, the Nusselt number for 3 mm channel is 0.04. Hence, there is a difference is 0.03. In this case, as well, the Nusselt number does not achieve a constant value and hence the boundary layer has not developed and the analysis in this case as well is said to be in the developing region of the channel.

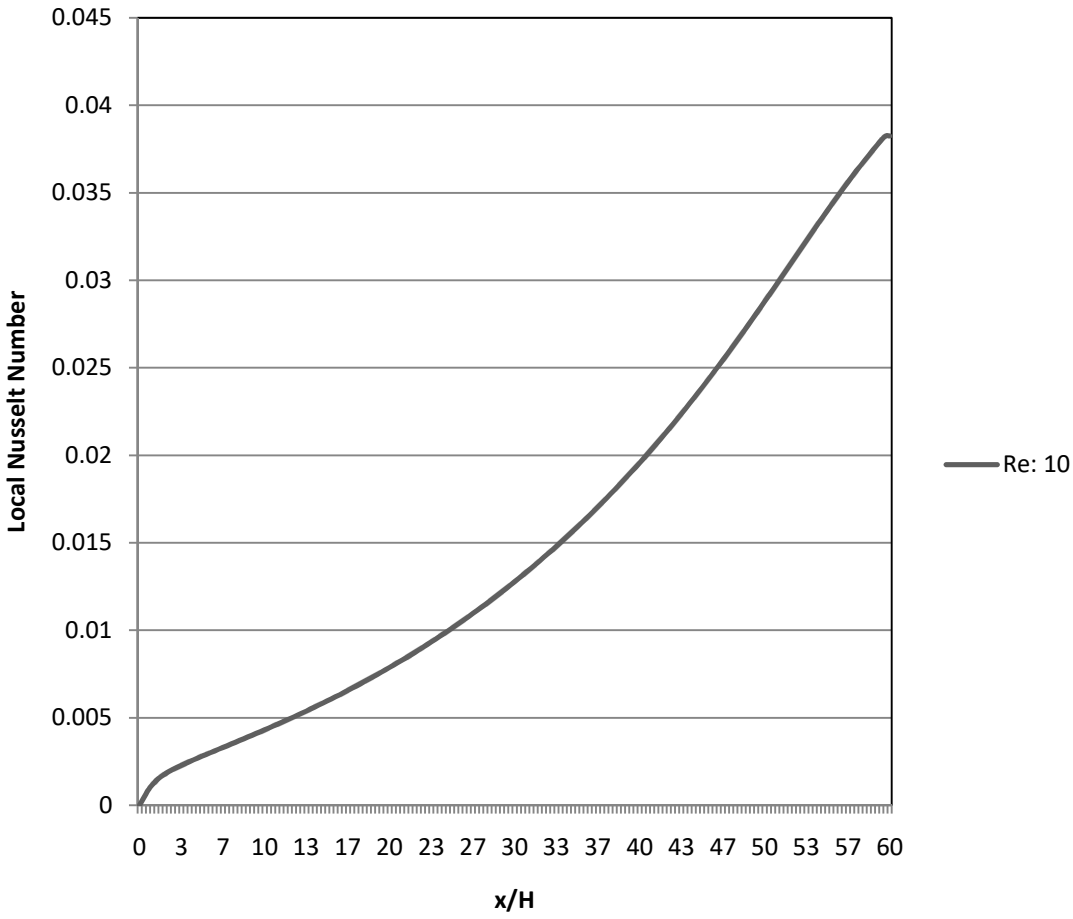

Figure 18: Local Nusselt number vs. x/H

For higher Reynolds numbers it can be said that the plot of Nusselt number is in the entrance region. If in these cases the channel length is increased, the Nusselt number will go on increasing until the thermal boundary layer develops as well as the heat transferred, as is shown in the following figures where the channel of length 100 mm is studied. Furthermore, the low value of Nusselt number suggests that conduction dominates the convection heat transfer in the entrance region, while as the thermal boundary layer develops the Nusselt number reaches unity, where the effect of conduction and convection is equal.

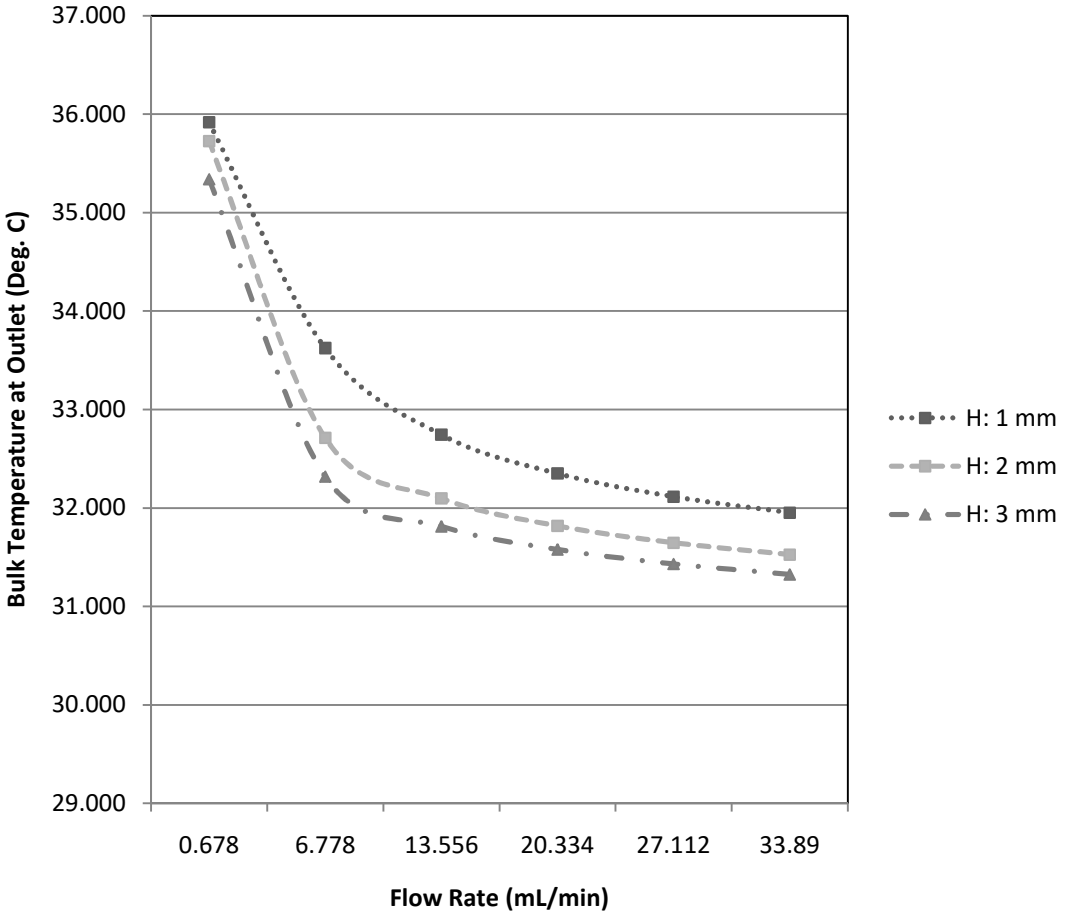

Figure 19: Bulk Temperature at outlet vs. flow rate

Above figure shows the variation of the bulk temperature at the outlet for various flow rates as a function of channel height. There is a decreasing trend in the temperature at the outlet with increasing flow rates, as is expected because the fluid a high velocity is unable to carry as much energy as the fluid at low velocity. Further, the temperature goes on decreasing with the increasing channel height. For a ration of Tiso / Tin = 1.2, there is not much difference in the temperature for all the configurations. However, if the wall temperature is increased further than a considerable difference can be seen in the temperature at the outlet. The difference in the inlet temperature and the outlet temperature is shown in the figure below. As can be seen from the figure below the analysis was done for flow rates ranging from 0.678 mL/min to 33.9 mL/min. As can be seen from the figure, increasing the

fin height a decreasing trend in outlet temperature is observed. The maximum temperature difference is observed to be 6 °C. Nevertheless, the temperature drops of 2 mm and 3 mm are close and comparable to each other.

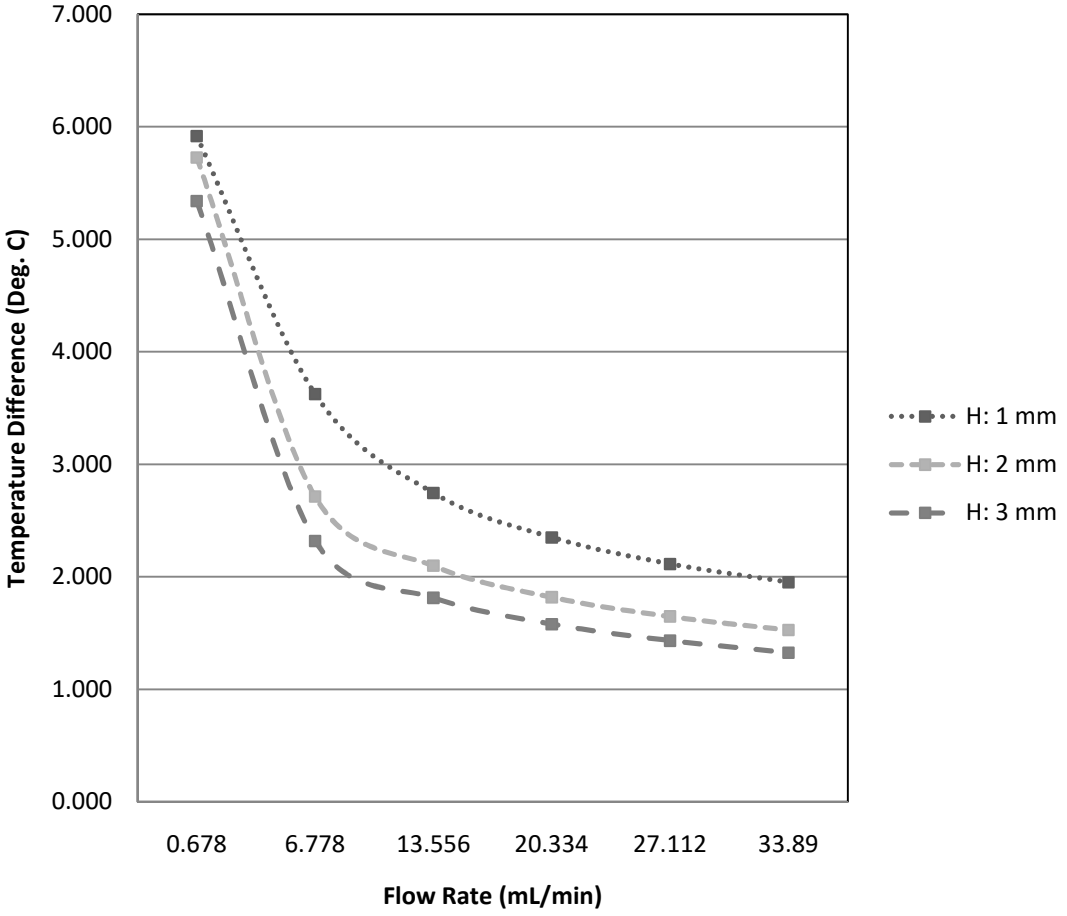

Figure 20: Temperature difference vs. flow rate

3.2.2.2 Two-Dimensional Channel with Imposed Heat Flux

The following are the results obtained for conjugate heat transfer. The heat flux incident is 55 kW / m^2. The initial length of the channel is 60 mm and the channel height is 1 mm. The figure below shows the variation of the bulk temperature at the outlet. As is expected the temperature at outlet decreases with increasing Reynolds number. The drop in temperature is more in the case of 1 mm channel. The performance of the all the three configurations is quite close and the temperature drop achieved by 2 mm and 3 mm channels, however, fall below the performance o 1 mm channel for the same flow rate.

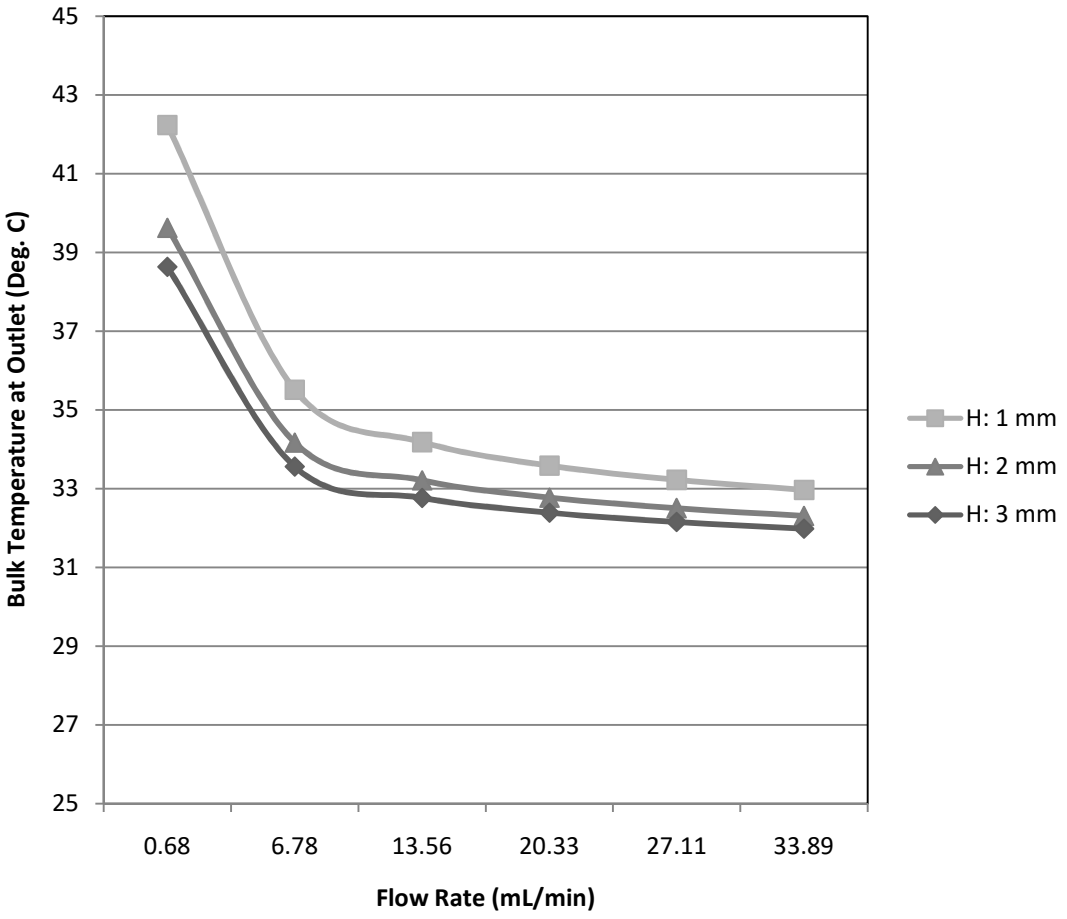

Figure 21: Bulk Temperature at outlet vs. Reynolds number

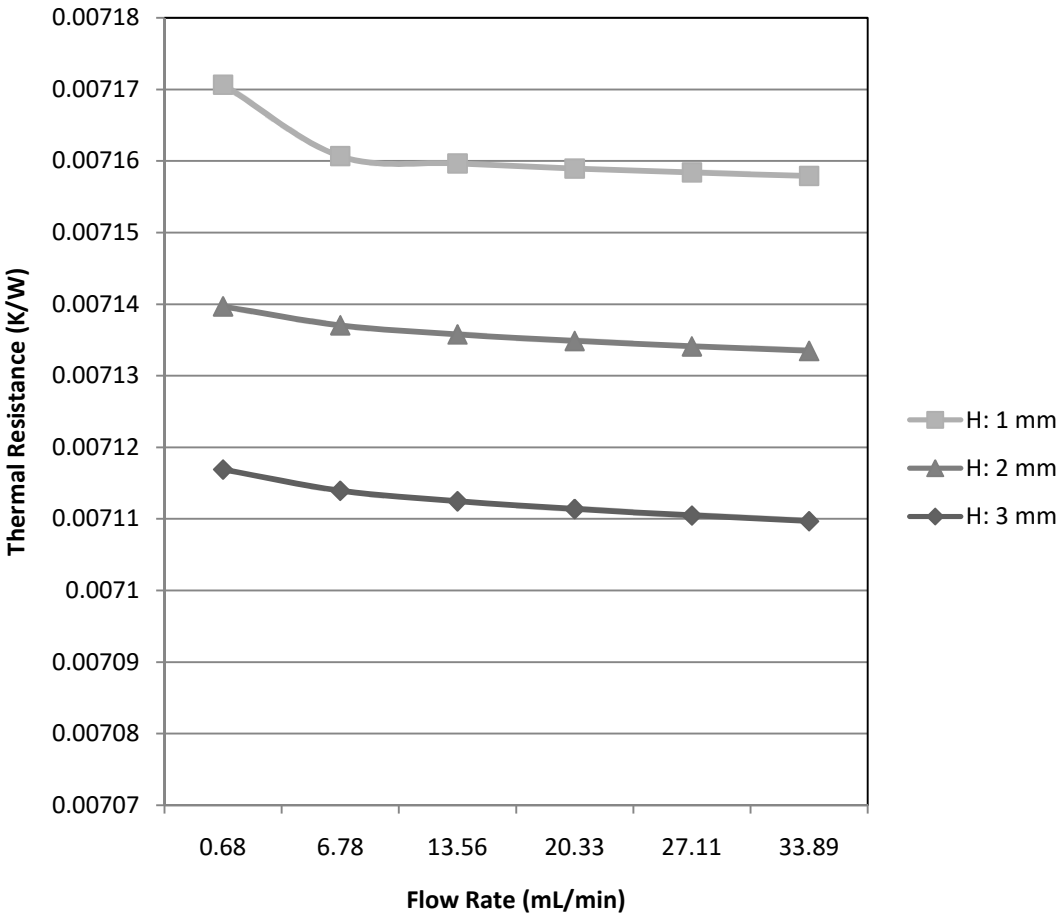

Figure 22: Thermal resistance vs. flow rate

The following formula gives the overall thermal resistance θ:

$$\boldsymbol{\theta} = \frac{(\boldsymbol{Tmax} - \boldsymbol{Tin})}{\boldsymbol{Q}}$$

Where, $\boldsymbol{Q = q\ x\ A}$

In addition, the T_{max} and T_{in} are the maximum bottom temperature and inlet fluid temperature respectively. Q is the total heat generated, q is the incident heat flux and A is the incident area. Figure 16 shows the effect of channel height on the thermal resistance. The decrease in thermal resistance is less than 1% when channel height is increased from 1 mm to 2 mm and further to 3 mm.

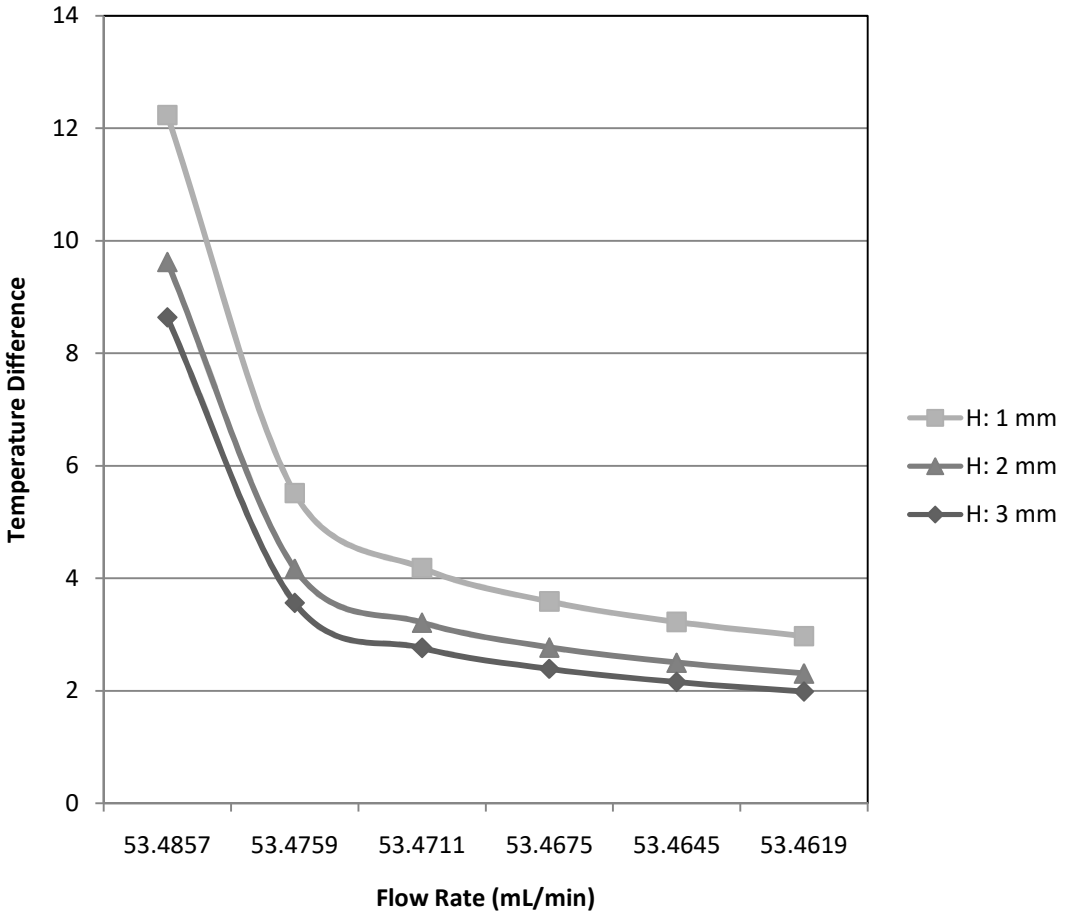

Figure 23: Temperature difference vs. flow rate

The following figure shows the variation of local Nusselt number with non-dimensional axial length. The trend is similar as seen for the cases before. The Nusselt number is plotted as a function of Reynolds numbers from 100 to 500. With increasing Reynolds number, the Nusselt number goes on increasing, which shows that the thermal boundary layer has not developed and the heat transferred will go on increasing with increasing length of the channel. After the initial entrance region, the Nusselt number plot lines are almost parallel to each other for various Reynolds numbers. Moreover, the overall Nusselt number is maximum for Reynolds number of 500 and is equal to 5.8. This suggests that the maximum heat is removed from the channel with Reynolds number of 500. Furthermore, this also suggests that for lower flow rate that is for lower Reynolds numbers the thermal boundary

layer will develop earlier than for higher flow rates. Therefore, while selecting the channel for heat sinks, the length of the channel and the pressure drop are one of the most important factors. As the length of the channel goes on increasing, the higher flow rates will provide higher heat transfer rate, however, as seen earlier the pressure drop will go on increasing with gradient more steep than the Nusselt number.

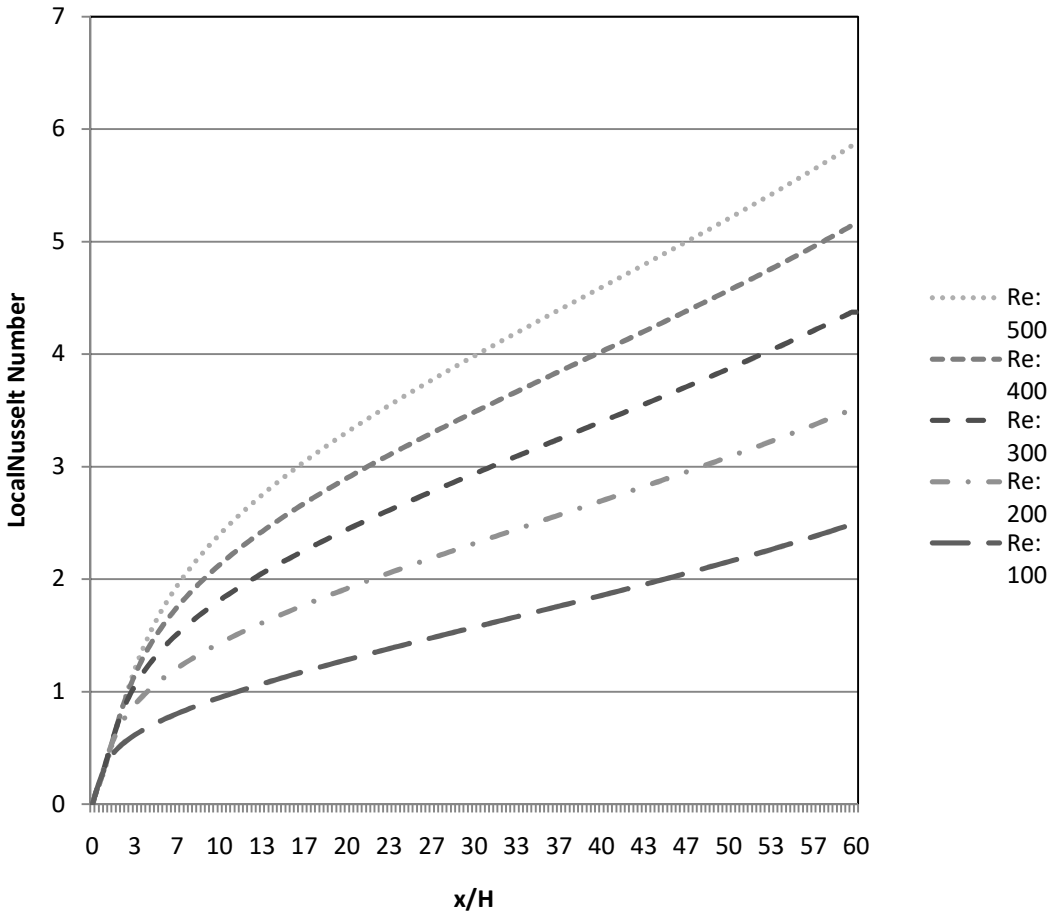

Figure 24: Local Nusselt number vs. x/H, L: 60 mm for imposed heat flux

The result discussed further are for the channel of length 100 mm and with three variations in height of 1 mm, 2 mm and 3 mm. Similar results as for 60 mm channel length will be considered. It is to be expected that most of the flows will be in the developing region with the exception of Reynolds number 10 flow in the channel of 1 mm height, which developed

in the 60 mm channel itself. Further, the variation of the bulk temperature at the outlet will also be studied, with varying flow rates. The bulk temperature at the outlet of the channels is expected to be increased than that for the smaller channels. As the temperatures at the outlet are increased, the difference in temperature is expected to increase. These expectations can be cross-checked using the following graphs and data.

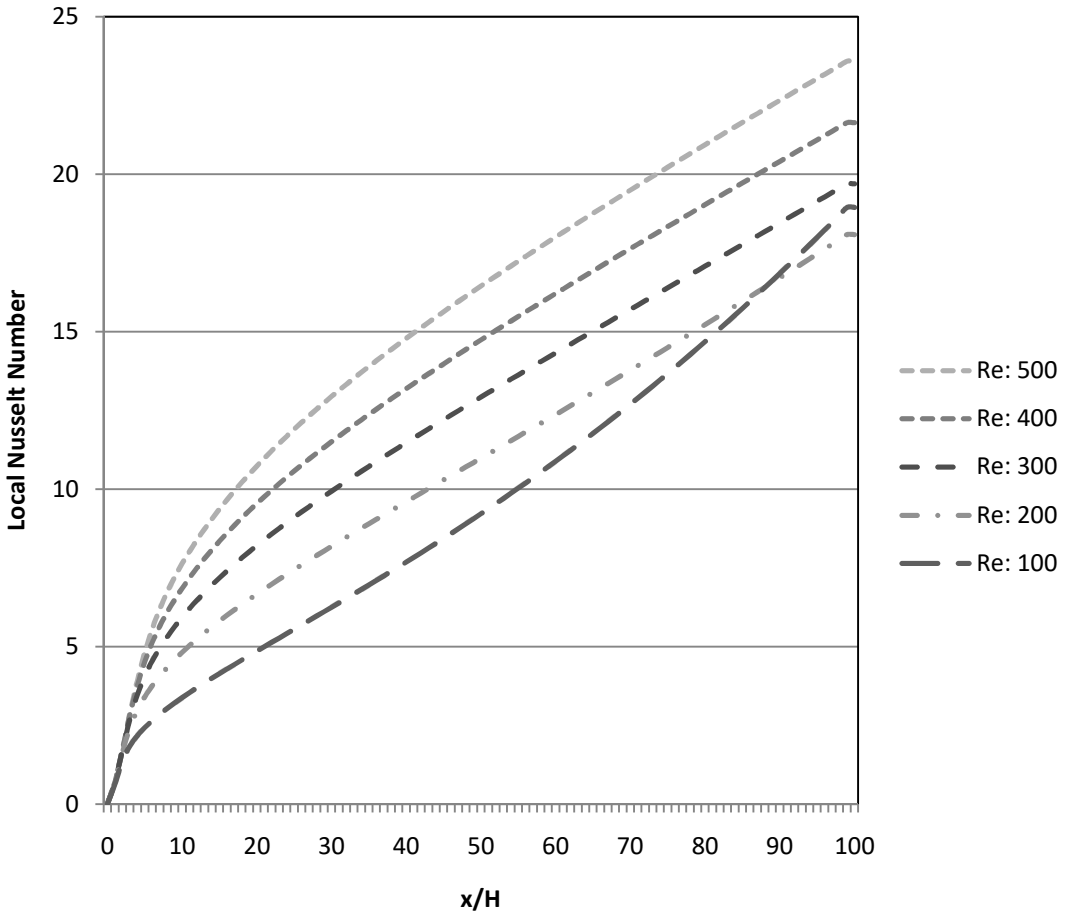

Figure 25: Local Nusselt number vs. x/H, L: 100 mm, H: 1mm

The above graph shows the variation local Nusselt number with non-dimensional axial length. The Nusselt number goes on decreasing with increasing Reynolds number. This is again because higher the velocity the lower energy the fluid can carry. However, as compared to the channel of length 60 mm there is a considerable increment in the Nusselt number for channel height of 1 mm. The increment is from almost 0.12 to just more than

0.14 for Reynolds number of 500.Similar is the case for other Reynolds numbers. Throughout the graph, it can be seen that the after the initial length of about 2.5 diameters the plot of Nusselt numbers for all the Reynolds numbers are parallel to each other. In addition, it can be seen that there is almost a linear increment in the Nusselt number for all Reynolds numbers after the initial length of 2.5-3 diameters. It can be inferred from the results that for even higher Reynolds numbers the Nusselt number will increase further, linearly. However, it should be noted that the increasing the Reynolds number will increase the pressure drop.

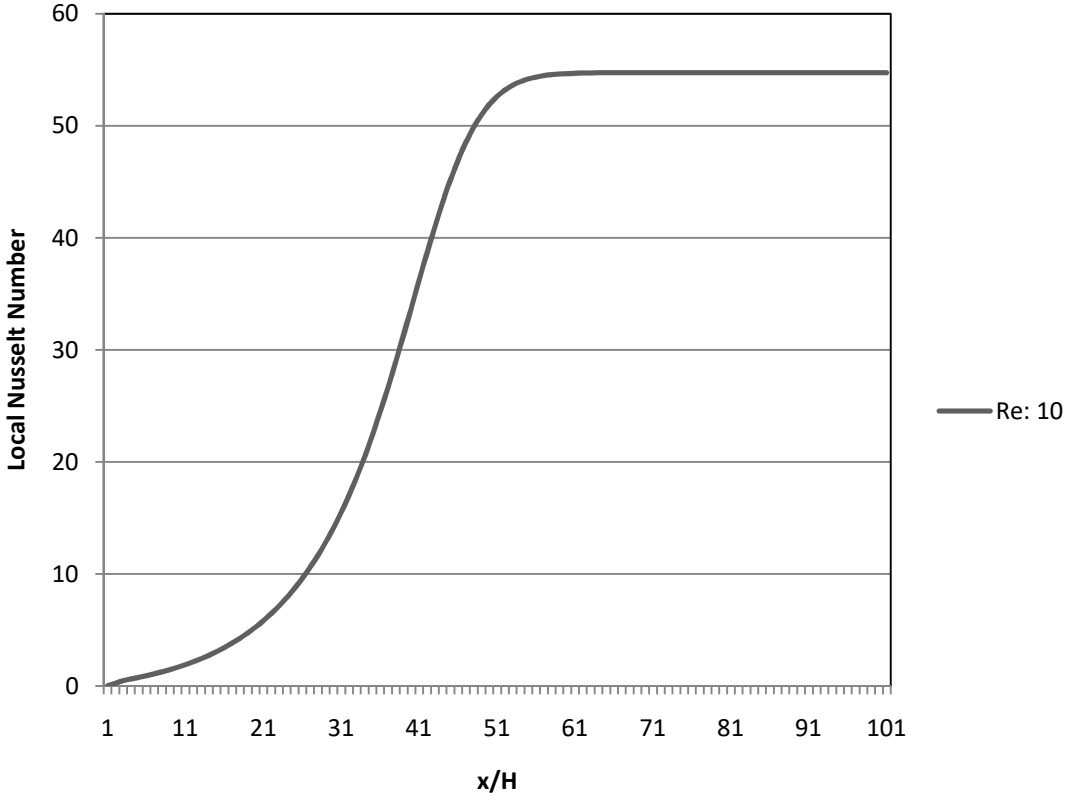

Figure 26: Local Nusselt number vs. x/H, L: 100 mm, H: 1 mm, Re: 10

The above figure shows the variation Nusselt number with non-dimensional axial length for a channel of length 100 mm and height 2 mm. Compared with Figure 18 the variation in Nusselt number is minor even with Reynolds number of 100. It is to be noted that the Nusselt number increment in previous cases for small Reynolds number was considerable. For the higher Reynolds numbers as well there is a minuscule change in Nusselt number. The

thermal boundary layer in this case as well as in the developing region. Channel with height 2 mm shows higher Nusselt numbers, which shows that heat transfer due to convection is dominant in the entrance region as compared to channel with height 1 mm. This can be attributed to the larger vertical dimension.

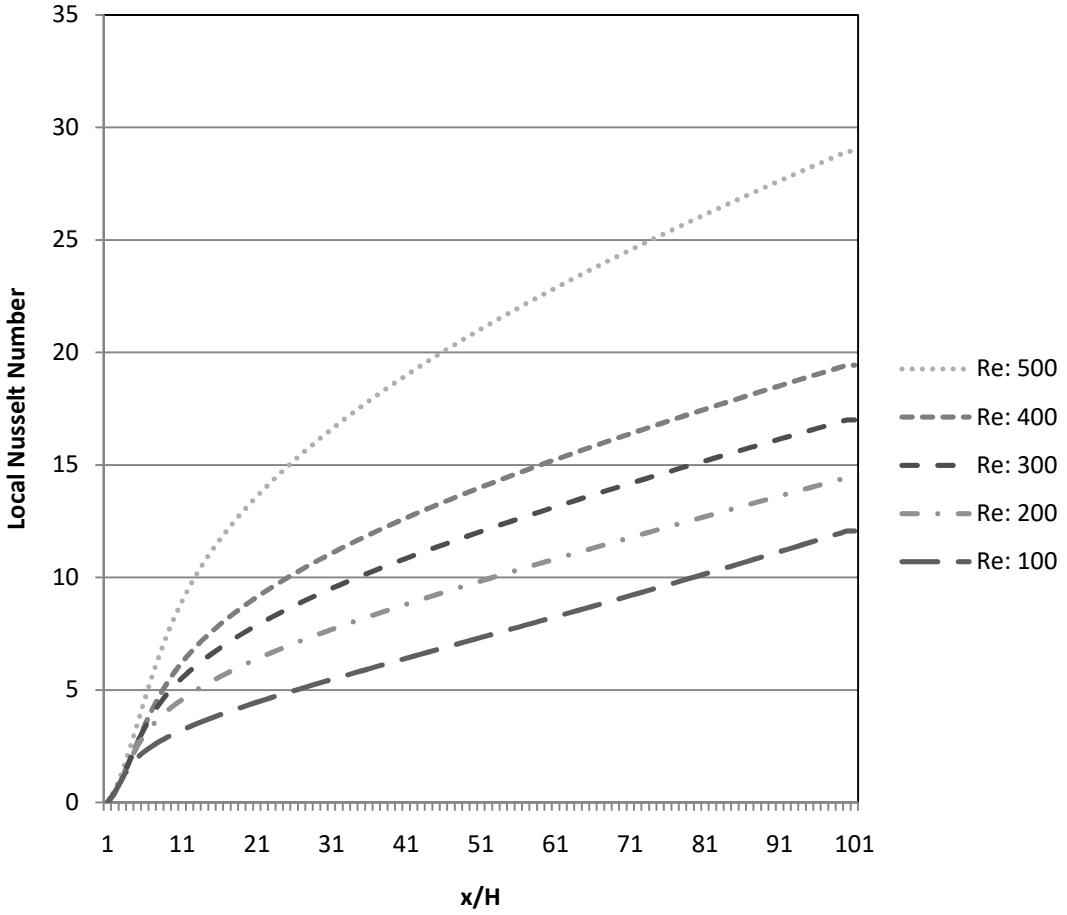

Figure 27: Local Nusselt number vs. x/H, Length: 100mm, Height: 2mm

3.2.2.3 Three-Dimensional Channel with Imposed Heat Flux

The results for the three-dimensional conjugate heat transfer are shown below. The temperature drop, the bulk temperature at the outlet and the thermal resistance are analyzed for various Reynolds numbers and fin heights. It is concluded from the analysis of two-dimensional channels that the heat transferred with 0.69 mL/min is low. Hence, for the

analysis of three-dimensional channel 0.69 mL/min is not considered. The computations in this section are done for three configurations with Reynolds numbers varying from 100 to 500. The bottom plate thickness 5mm and the channel wall thickness is 1 mm. Here, the purpose is to examine the maximum heat flux with the change in channel height. There is no restriction on the temperature difference between inlet and outlet. Hence, the maximum allowable heat flux that can be imposed can be examined. In the Fluid Performance section, the trend of pressure drop with channel width has been shown, the temperature also shows a similar trend.

The following figure shows the variation of the bulk temperature for varying Reynolds numbers as a function of the fin height.

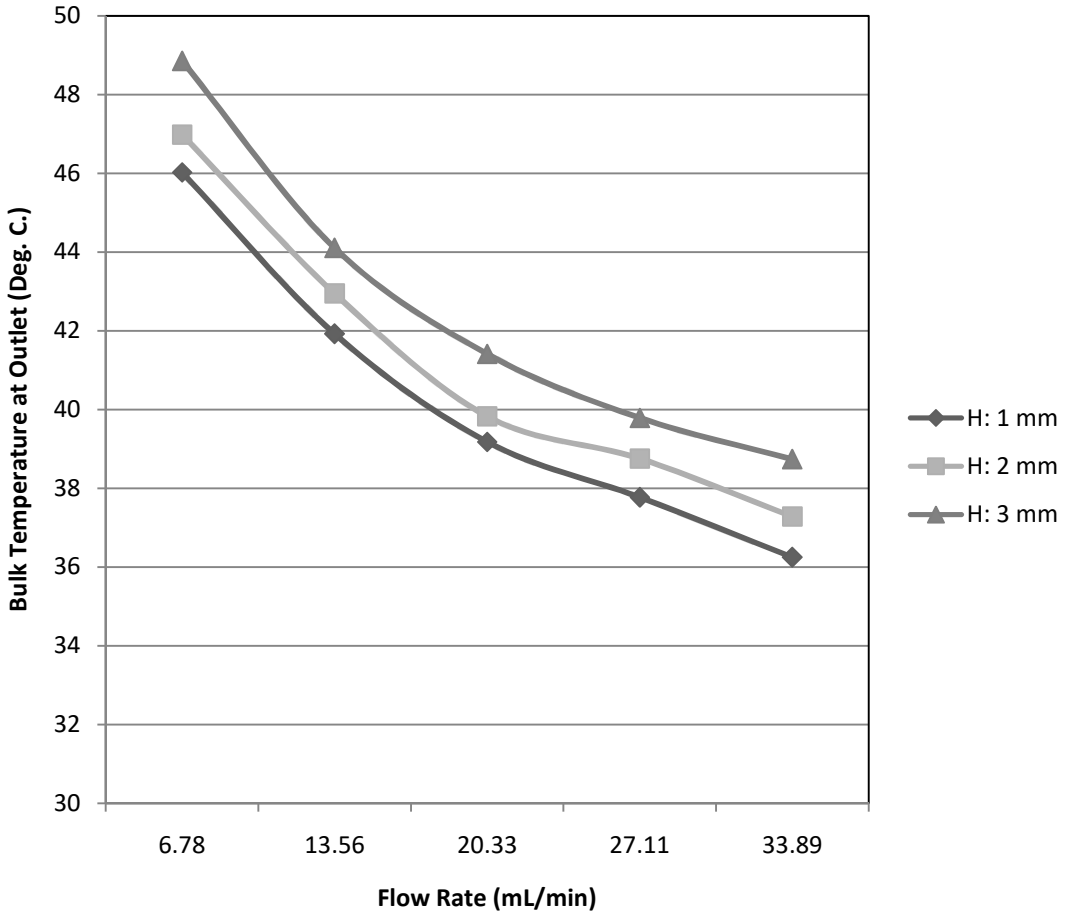

Figure 28: Bulk temperature at outlet vs. flow rate

The maximum temperature obtained at the outlet is 48.84°C for the fin height of 3 mm and the lowest flow rate of 6.78 mL/min. While the minimum temperature is obtained for, the 1 mm fin height configuration with maximum flow rate of 33.9 mL/min and is equal to 36.24°C. The gradient for temperature drop is similar in all the three cases. Higher the temperature higher is the energy carried by the fluid. The trend of variation of the bulk temperature at the outlet with varying channel height is opposite to the pressure drop variation with increasing flow rates.

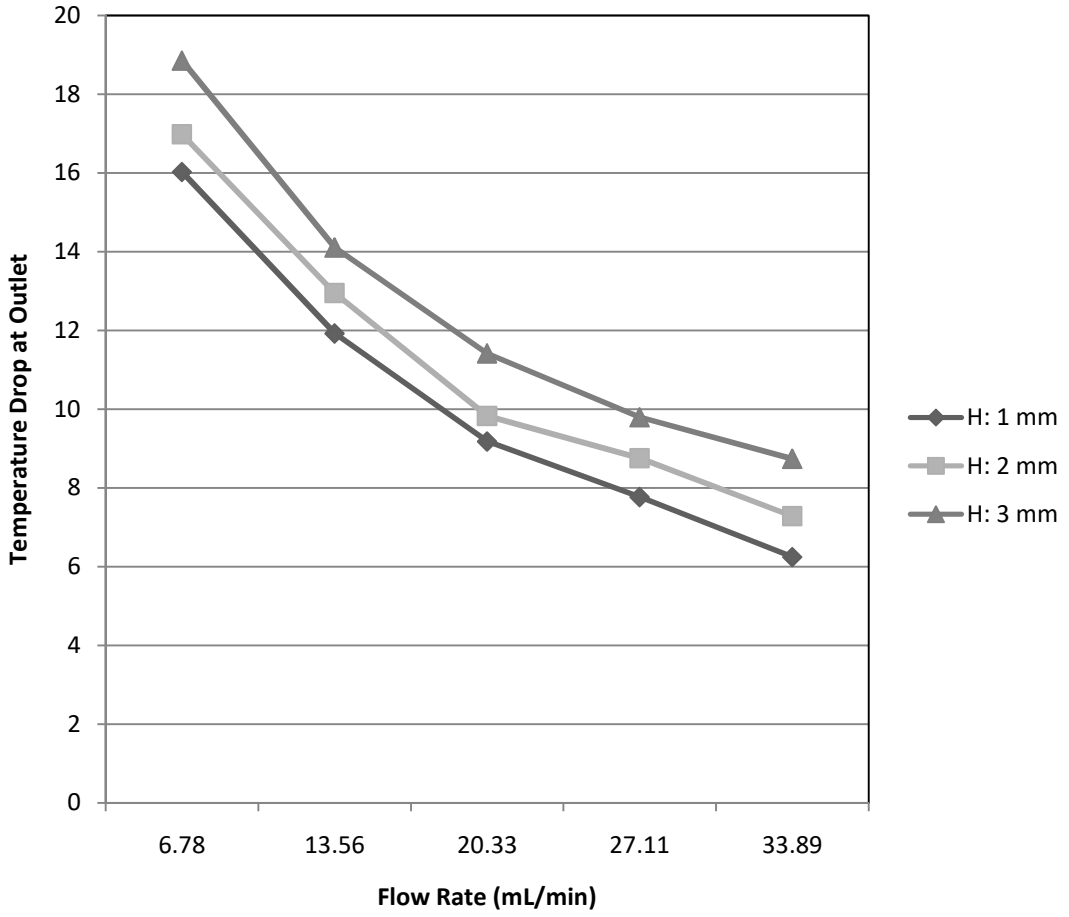

Figure29: Temperature drop vs. flow rate for three-dimensional channel

The maximum temperature at the outlet is for the channel with 3 mm height and for minimum flow rate 6.78 mL/min. However, the maximum heat transferred is with the channel of 3 mm with the maximum flow rate of 33.89 mL/min, which is 21.249 W. The imposed heat flux is 70 W/cm^2, with the imposed are of 3 mm by 100 mm. Therefore, the heat flux is 210 W on the channel. Figures 30 and 31 show the variation of temperature drop and the heat transferred through the channel. The trend of the bulk temperature is similar to the cases seen previously. The trend of heat transfer in the channel suggests that the heat removal capacity is better in a rectangular channel than a square channel. Therefore, it can be concluded that with increasing channel cross-section aspect ratio and flow rate the heat transferred will go on increasing

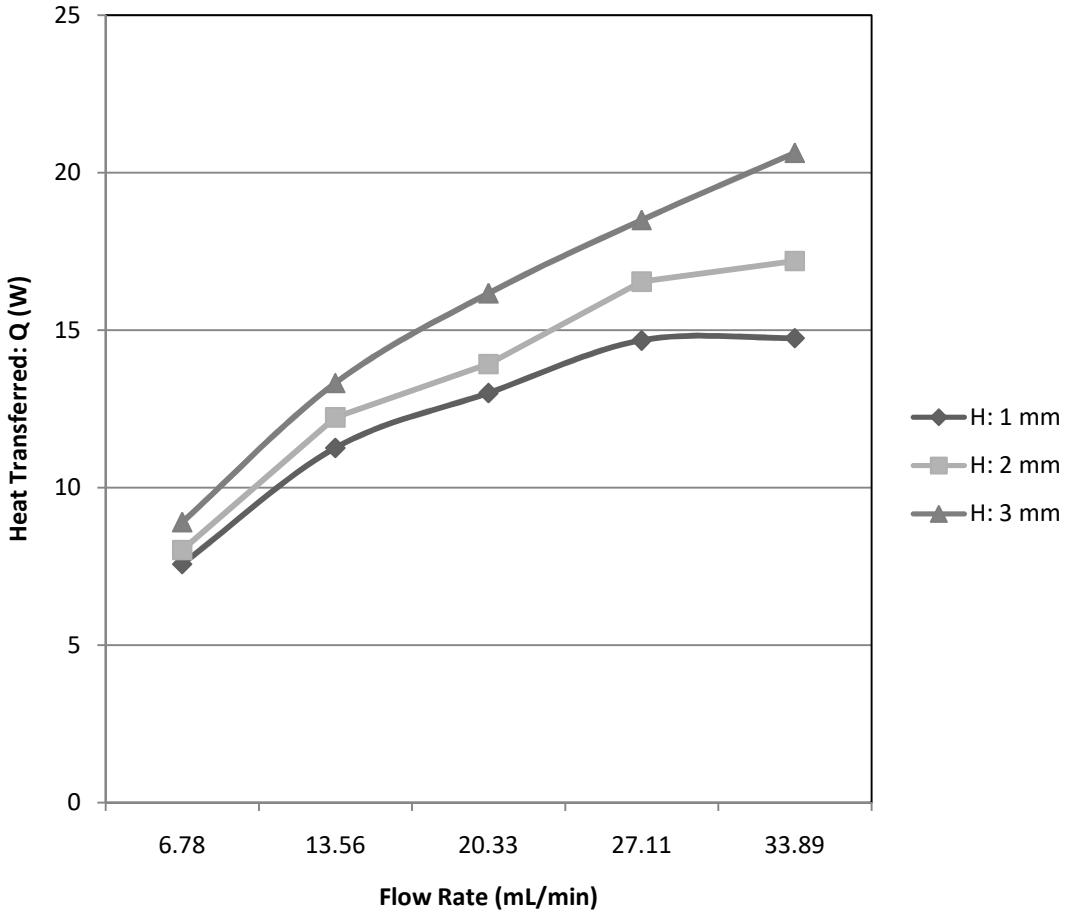

Figure 30: Heat transferred vs. flow rate for three-dimensional channel

The following figure shows the variation of thermal resistance with respect to the fin height, for flow rates ranging between 6.78 to 33.89 mL/min. Thermal resistance is the measure of temperature difference by which a system resists heat flow. It can be seen from the figure that the highest resistance is for the case corresponding to Reynolds number of 100 and fin height 1 mm. The minimum value of thermal resistance is for the case of highest flow rate for fin height of 3mm. Moreover, it can be seen from the figure that thermal resistance is almost independent of the flow rate and highly dependent on the fin height. Furthermore, a conclusion can be drawn that the thermal resistance ultimately depends on the channel cross-section aspect ratio.

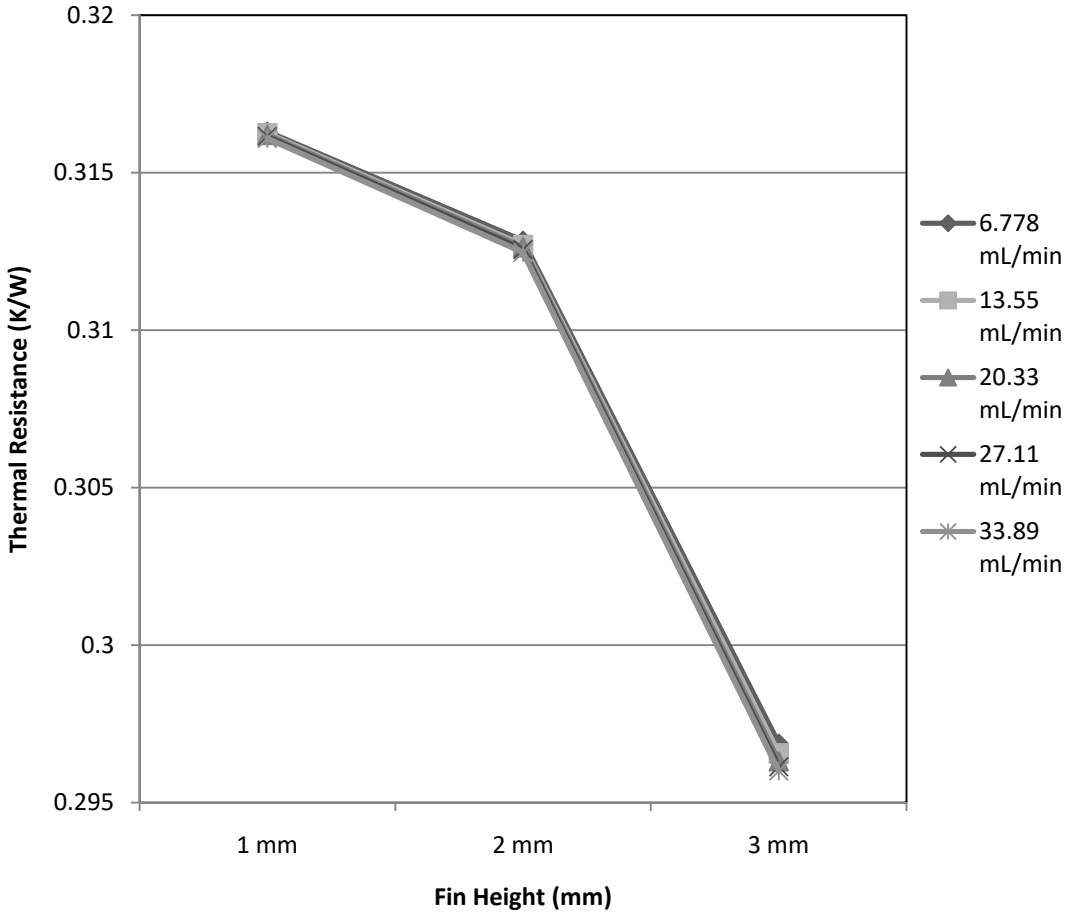

Figure 29: Thermal resistance vs. fin height for three-dimensional channel

The base temperature of the heat sink is an important parameter to be analyzed. Figure 33 shows the variation of the base temperature of the heat sink with varying flow rates. The minimum base temperature is obtained for a flow rate of 33.89 mL/min with the fin height of 3 mm. For example, this case simulates the situation when heat is generated by a processor. The best performance is observed with fin height of 3 mm and flow rate of 33 mL.min. A minimum temperature of 80.36 ^{o}C is obtained with 3 mm fin and flow rate of 33mL/min. The maximum temperature drop is observed for fin height of 3mm as well which is 12.48 ^{o}C. The performance of the other two configurations is slightly lower however it is comparable.

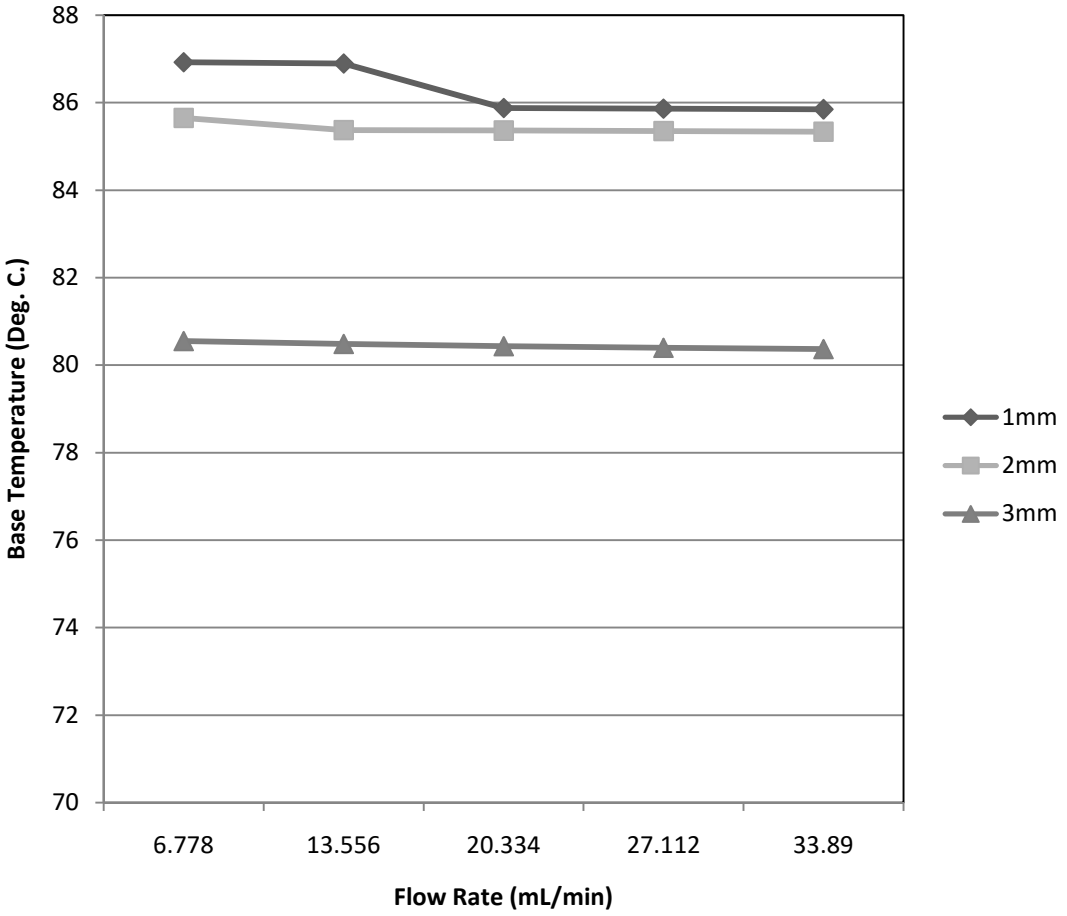

Figure 30: Base temperature vs. flow rate for three-dimensional channel

The final investigation is carried out dimensionless parameters to better under the thermal performance of the heat sink under study. Nusselt number vs. Reynolds number plot is shown in the following figure. Nusselt number is an important parameter as it shows which mode of heat transfer is dominant in the channel. It can be seen that for a heat sink with 3mm fin height the Nusselt number is the greatest for Reynolds number of 500. A larger number of Nusselt number denotes that convection heat transfer is dominant while a lower Nusselt number denotes conduction is dominant.

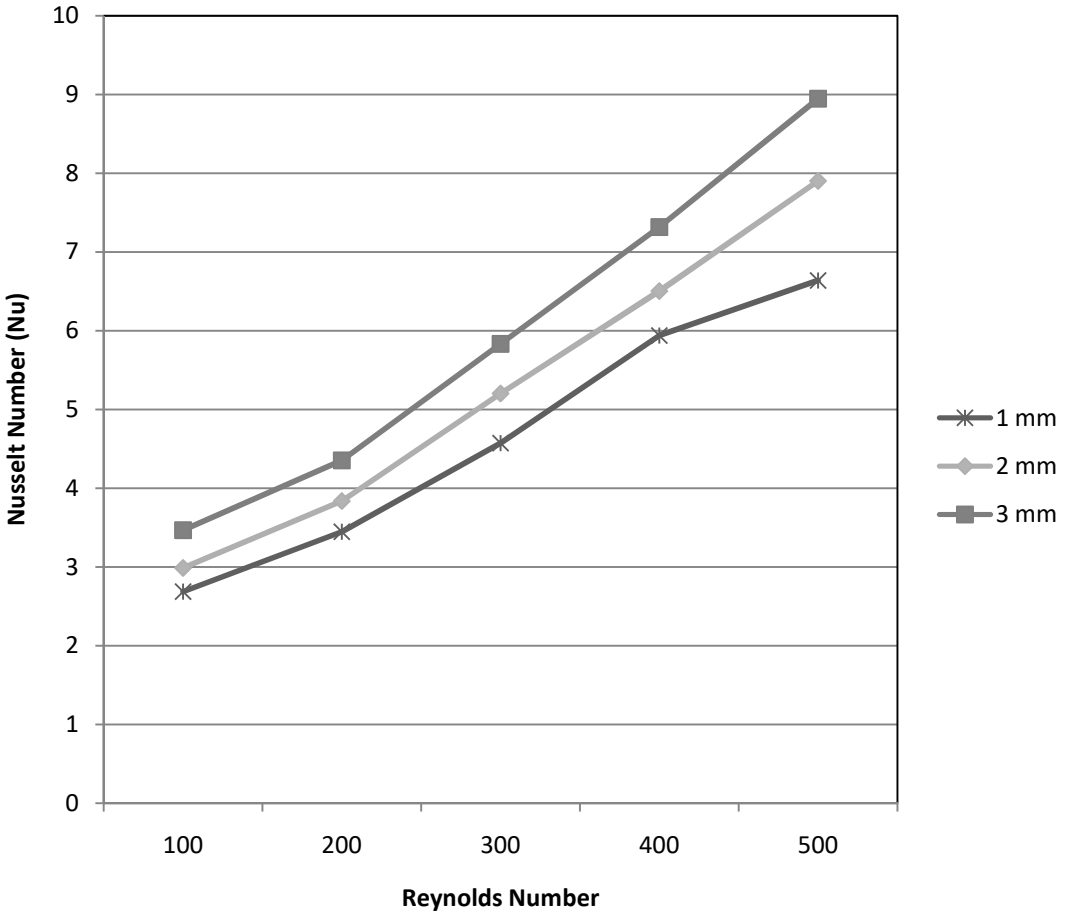

Figure 31: Nusselt Number vs. Reynolds Number

As can be seen from the trend of Nusselt number, it goes on increasing with increase in with Reynolds number and fin height. This suggests that the convection heat transfer is dominant

as the fin height is increased for the same Reynolds number. The Nusselt number is calculated by the following formula:

$$Nu = \frac{Qw * D}{k * (Tw - Tm)}$$

where Qw is the heat flux

D is the hydraulic diameter

k is the thermal conductivity of water

Tw and Tm are the wall and mixing cup temperature

Chapter 4: Conclusions and Future Work

4.1 Conclusion

This work presents the analysis of minichannel heat sinks with a low aspect ratio of the order of 0.01. Thermal transport in two and three-dimensional channels with isothermal surfaces and imposed heat flux is simulated numerically and the results are analyzed.

In the first part of the thesis, the design aspects of minichannels were studied from previous studies. This section reviews the various designs of minichannels done by researchers prior to doing this study. Various other methods for enhancing the heat transfer through minichannels were studied.

In the mathematical and numerical modeling section the design of the channels under consideration, equations solved, the assumptions made and the boundary conditions are explained. Further, the validation of the code is shown in the validation section with other studies done numerically as well as with theoretical and with co-relations. The overall error is less 10 % for all the quantities.

In the later sections, the performance of two and three-dimensional channels are analyzed, for both fluid and thermal performance. In all six configurations of two-dimensional channels are considered and three-configurations of three-dimensional channels are considered. A heat flux of 55 $W/m^2$is imposed on the bottom surface. Transport in six configurations is analyzed. The maximum heat transferred is 14.15 W with the 100 mm channel and height of 1 mm. The thermal resistance goes on decreasing with increasing flow

rates and the channel height. The minimum thermal resistance is 0.00711 for a channel with height 3 mm and the flow rate is 33.89 mL/min. However, the decrease in thermal resistance is less than 1% when channel height is increased from 1 mm to 2 mm and further to 3 mm.

On the three-dimensional channel, a heat flux of 70 $W/cm^2$is applied on the bottom of the channel. For a channel with hydraulic diameter 1 mm the heat transferred is 21.249 W. Moreover, the thermal resistance goes on decreasing with increasing flow rates. Furthermore, it is evident that the most effective channel for heat removal is the channel with height 3 mm. Therefore, it can be concluded that a narrower channel, that is a channel of which the height is greater than the width is the most effective geometry for heat removal and can be used in various applications.

Furthermore, it is concluded that using advanced fluids such nanofluids can be used as working fluids in heat sinks to increase the heat transferred many folds. However, using simpler and cheap fluids like distilled water are chosen over nanofluids is the disadvantages of using such fluid, for example, high maintenance, deposition on the surface of the channels etc. Moreover, this study shows that there is a lot of potentials for water to be used as working fluids in many applications.

4.2 Future Work

Most of the work done on analysis of thermal transport in minichannels is steady state. Furthermore, most numerical analysis works assume no body forces acting on the fluid and consider straight minichannels without any changes in geometry. In future work can be done on these aspects. Moreover, the use and effectiveness of other easily available fluids like ethyl alcohol should be should be studied and explored, rather than using nano-fluids of which the performance is still ambiguous and are highly costly to use and maintain.

Bibliography

[1] Jajja S., Ali W., Ali H. and Ali A., “Water cooled minichannel heat sinks for microprocessor cooling: Effect of fin spacing,” *Applied Thermal Engineering,* vol. 64, no. 1-2, pp. 76-82, 2014.

[2] Xie X. L., He Z. J., He Y. L. and Tao W. Q., “Numerical study of laminar heat transfer and pressure drop characteristics in a water-cooled minichannel heat sink,” *Applied Thermal Engineering,* 2008.

[3] Kandlikar S. G. and Dharaiya V. V., “A numerical study to predict the effects of structured roughness elements on pressure drop and heat transfer enhancement in minichannels and microchannels,” in *ASME 2011 International Mechanical Engineering Congress and Exposition, Volume 10, pages 1007-016*, Denver, Colorado, 2011.

[4] Kandlikar S. G. and Balasubramanian P., “An extension of the flow boiling correlation to transition, laminar, and deep laminar flows in minichannels and microchannels,” *Heat Transfer Engineering,* vol. 25, no. 3, pp. 86-93, 2004.

[5] Xuan Y. and Li Q., “Heat transfer enhancement of nanofluids,” *International Journal of Heat and Fluid Flow,* vol. 21, no. 1, pp. 58-64, 2000.

[6] Choi S., Zhang Z., Yu W., Lockwood F. and Grulke E., “Anomalous thermal conductivity enhancement in nanotube suspensions,” *Applied Physics Letters,* vol. 79, no. 14, pp. 2252-2254, 2001.

[7] Kandlikar S. G., “Microchannels and minichannels - History, terminology, classification and current research needs,” in *First International Conference on Microchannels and Minichannels*, New York, 2003.

[8] Vembuli V., *Experimental investigation of minichannel heat sinks for electronic cooling applications,* New Brunswick, NJ, 2015.

[9] Thakur S. and Shyy W., “Some implementational issues of convection schemes for finite-volume formulations,” *Numerical Heat Transfer,* 1993.

[10] Patankar S. V., Numerical Heat Transfer and Fluid Flow, New York: McGraw Hill Book Company, 1980.

[11] Kandlikar S. G., Garimella S., Li D., Colin S. and King M. R., Heat Transfer and Fluid Flow in Minichannels and Microchannels, Elsevier Ltd., 2006.

[12] Conti A., Lorenzini G., and Jaluria Y., "Transient conjugate heat transfer in straight microchannels," *International Journal of Heat and Mass Transfer,* vol. 55, no. 25-26, pp. 7532-7543, 2012.

[13] Jaluria Y. and Torrance K. E., Computational Heat Transfer, New York: Hemisphere Publishing Company, 1986.

[14] Jaluria Y., Design and Optimization of Thermal Systems, New York: McGraw-Hill, 1998.

[15] Incropera. F. P., "Convection heat transfer in electronic equipment cooling," *ASME Journal of Heat Transfer,* vol. 110, no. 4b, pp. 1097-1111, 1988.

[16] Dewan A. and Srivastava P., "A review of heat transfer enhancement through flow disruption in a microchannel," *Journal of Thermal Science,* vol. 24, no. 3, pp. 203-214, 2015.

[17] Ferziger J. H. and Peric M., Computational Methods for Fluid Dynamics, New York: Springer, 2002.

[18] Khanafer K. and Vafai K., "A critical synthesis of thermophysical characteristics of nanofluids," *International Journal of Heat and Mass Transfer,* vol. 54, no. 19-20, pp. 4155-4458, 2011.

[19] Schmitt D. J. and Kandlikar S. G., "Effects of repeating microstructures on pressure drop in rectangular minichannels," in *ASME 3rd International Conference on Microchannels and Minichannels*, Toronto, Ontario, Canada, 2005.

[20] Shao B., Wang L., Chen H. and Li J., "Optimization and numerical simulation of multi-layer microchannel heat sink," *Procedia Engineering,* vol. 31, pp. 928-933, 2012.

[21] Steinke M. E. and Kandlikar S. G., "Single phase heat transfer enhancement techniques in microchannel and minichannel flows," in *ASME 2nd International Conference on Microchannels and Minichannels*, Rochester, New York, 2004.

[22] Versteeg H. K. and Malalasekera W., An Introduction to Computational Fluid Dynamics, New York: John Wiley & Sons Inc., 1995.

[23] Zhang J., Jaluria Y., Prakash S., and Lin L., "An experimental study on the effect of configuration of multiple microchannels on heat removal for electronic cooling," in *Proceedings of IHTC -14*, Washington DC, 2010.

[24] Sun Z. and Jaluria Y., *Numerical modeling of nitrogen slip flow in long rectangular microchannels,* New Brunswick, New Jersey, 2009.